Geomorphology 458 (2024) 109232

Contents lists available at ScienceDirect

Geomorphology

journal homepage: www.journals.elsevier.com/geomorphology

Holocene relative sea-level variation and coastal changes in the Bay of Cádiz: New insights on the influence of local subsidence and glacial hydro-isostatic adjustments

C. Caporizzo [a], F.J. Gracia [b], C. Martín-Puertas [c], G. Mattei [d,*], P. Stocchi [e,f,g], P.P.C. Aucelli [d]

[a] Department of Engineering, Università Telematica Pegaso, Italy
[b] Department of Earth Sciences, Facultad de Ciencias del Mar y Ambientales, Universidad de Cádiz, Spain
[c] Department of Geography, Royal Holloway University of London, United Kingdom
[d] Department of Science and Technologies, Università degli Studi di Napoli Parthenope, Italy
[e] NIOZ - Royal Netherlands Institute for Sea Research, Coastal Systems (TX), Utrecht University, the Netherlands
[f] Department of Pure and Applied Sciences, Università degli Studi di Urbino, Italy
[g] Institute for Climate Change Solutions, Italy

ARTICLE INFO

Keywords:
Relative sea-level changes
Salt marsh
Coastal changes
Glacio-hydro-isostatic adjustment models
Southern Spain

ABSTRACT

The Bay of Cádiz is located in South-western Spain (Andalusia region) and constitutes an example of a typical estuarine salt marsh environment. In this study we reconstruct its Holocene morpho-evolution and relative sea-level change history by assembling a geodatabase of geological sea-level markers derived from boreholes and bibliographic data, standardized to the most recent international guidelines for RSL studies. The identified high-precision sea-level index points were compared to a number of new site-specific glacio-hydro-isostatic adjustment (GIA) models in order to disentangle potential components which influenced the sea-level evolution and finally obtain the vertical displacement (VD) trends that affect this coastal area by using a Bayesian statistical approach including Monte Carlo simulations. In general, the whole area was affected by overall subsidence related to the local sediment compaction, which had an impact on the morpho-evolution of the different zones with a variable entity and completely outclassed the GIA-driven component. Between 6.7 and 3.0 ka BP, the northern sector of the bay was characterized by subsidence rates of about - 0.65 mm/yr while, during the last 3.0 ka, the general trend appears to be homogeneous for both the main sectors of the bay with an average subsidence rate of - 1.6 mm/yr. The Holocene RSL curve from the Gulf of Cádiz aligns with past reconstructions, revealing subtle differential trends in subsidence rates in the northern and southern sectors of the Bay of Cádiz due to varying substratum.

1. Introduction

Coastal depositional environments are the most complete archives of the detailed history of relative sea-level (RSL) change in the last millennia as their vertical variability can be analysed to reconstruct the morpho-evolution of these low-lying areas in relation to global mean sea-level changes (MSL), glacial- and hydro-isostatic adjustments (hereafter GIA; Farrell and Clark, 1976; Peltier, 1976; Mitrovica and Peltier, 1993; Spada and Stocchi, 2007), and local vertical crustal displacements (Vacchi et al., 2016; Roy and Peltier, 2018a,Roy and Peltier, 2018b). Usually, a lithofacies model is created by analyzing well-distributed boreholes. This model not only outlines the distribution of sedimentary environments but also provides insights into how these environments have evolved over time (Nelson, 2015; Fagherazzi et al., 2020; Nageswara Rao et al., 2020).

In this context, salt marshes, which are brackish environments usually located close to large deltas, estuaries, and coastal lagoons, are particularly dynamic systems able to laterally expand, contract, and vertically accrete in response to sea-level rise (Rahman and Plater, 2014). Generally, it is possible to distinguish between two types of stratigraphic sea-level markers according to their relationship with the mean sea level, lower and upper salt marsh levels. While the lower salt marsh deposits are located between the MSL and the mean high water (MHW) and, consequently, subjected to inundation twice a day (Dyer

* Corresponding author.
E-mail address: gaia.mattei@uniparthenope.it (G. Mattei).

https://doi.org/10.1016/j.geomorph.2024.109232
Received 26 June 2023; Received in revised form 26 April 2024; Accepted 26 April 2024
Available online 8 May 2024

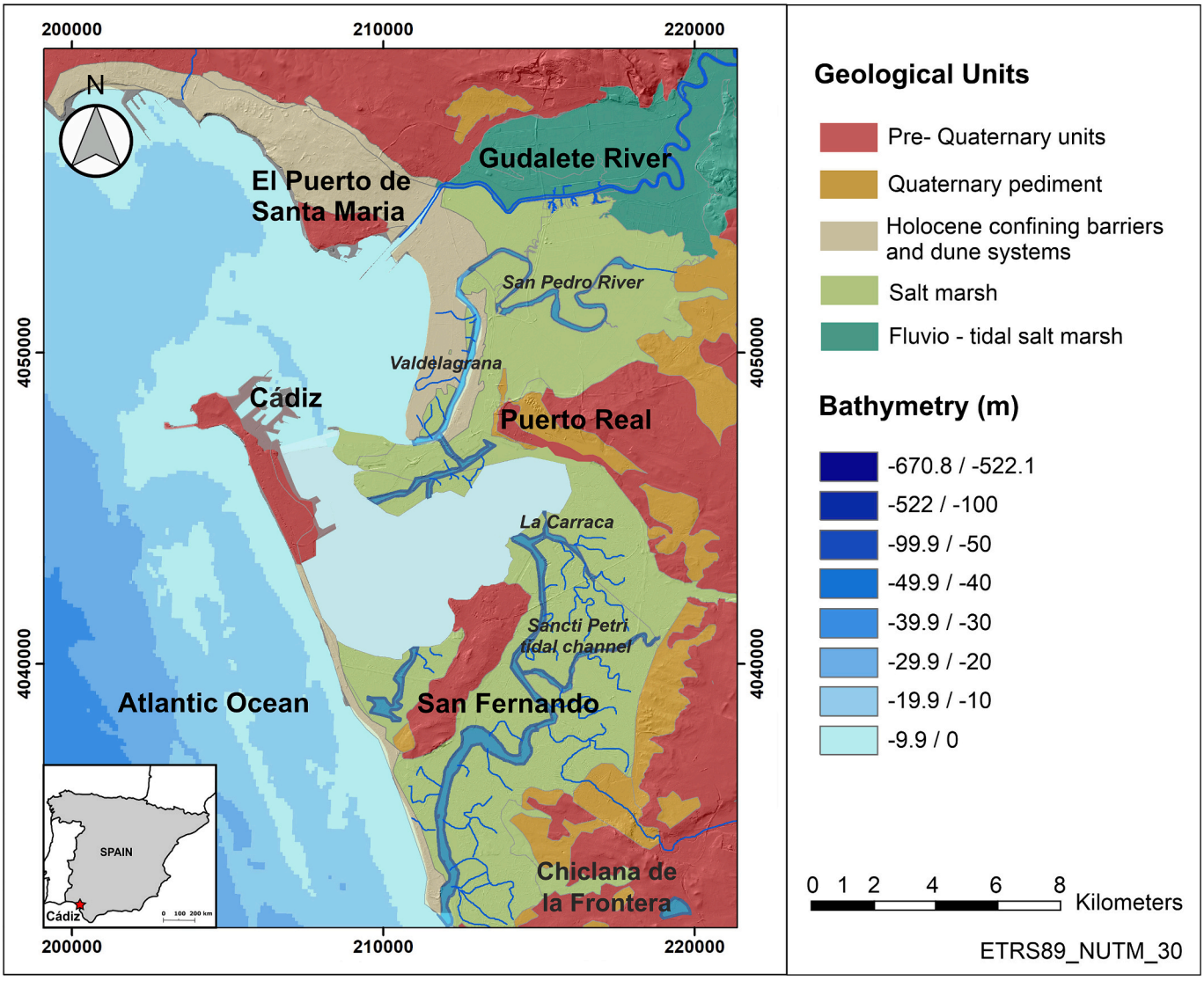

Fig. 1. Geological-geomorphological sketch of the study area.

et al., 2000), the upper salt marsh, which deposits form between the mean high-water neaps (MHWN) and the highest astronomical tide (HAT), receives tidal inundation only periodically, often twice a month. This strict relationship between the salt marsh deposits and the MSL makes the marsh samples reliable sea-level index points (SLIPs, Vacchi et al., 2016). However, this relationship depends on several factors, such as the tidal regime: macro and mesotidal marshes can adapt to sea level rise (SLR) more efficiently than microtidal marshes (Hofstede et al., 2018); and the rate of SLR – if it is too rapid marshes cannot face the changing conditions and become passively flooded (Kirwan et al., 2010; Best et al., 2018; Reed et al., 2020). Process-based models indicate that marshes would survive under relatively fast rates of SLR (>10 mm/yr) if sediment delivery to the coast is not restricted by either dams (Kirwan et al., 2016) or other factors and processes (e.g. land use changes) causing a decrease in sediment transport.

Geological sea-level markers with this high level of precision offer the unique opportunity to:

- Constrain/calibrate the numerical GIA models, which combine ice sheet chronologies (forcing) and solid Earth (response) models, provided that the non-GIA processes (tectonics, sediment compaction, etc.) are absent or known and therefore can be filtered out;
- Quantify the non-GIA processes by comparing data and GIA models, assuming that the a priori GIA models have been satisfactorily constrained by other independent RSL data;
- Apply statistical analysis to evaluate and calculate the risk of flooding related to the ongoing sea-level rise often exacerbated by vertical crustal deformations and subsidence, which is mainly related to sediment compaction in the case of well-developed coastal plains (Brain et al., 2015).

The coastal area of the Bay of Cadiz constitutes an example of long historical human occupation, started with the foundation of the first Phoenician colony of *Gadir* around the 1100 BCE (*Velleius Paterculus*, Hist. Rom. I.2.1–3; Ruiz Mata, 1999), of a typical estuarine salt marsh environment affected by notable historical changes that have conditioned the sedimentary evolution of emerged and submerged zones (Gutiérrez-Mas et al., 2009; Gracia et al., 2017; Caporizzo et al., 2020). However, the Late Holocene coastal evolution of this area has so far remained unclear and the RSL change studies have been practically lacking (Dabrio et al., 2000; Lobo et al., 2005). Given the distance from the LGM ice sheets, this area can be considered a "far-field" site with respect to the GIA processes, i.e. it is not directly affected by the ice-load-driven deformations, which cause the largest deviations from the eustatic trend (i.e. GMSL change) and that characterize the ice-proximal locations. In the case of the 'far field' areas (i.e. equatorial islands and the coastal areas located far from the sheets; Milne and Mitrovica, 2008; Spada and Stocchi, 2007; Kopp et al., 2015; Khan et al., 2015; Rovere

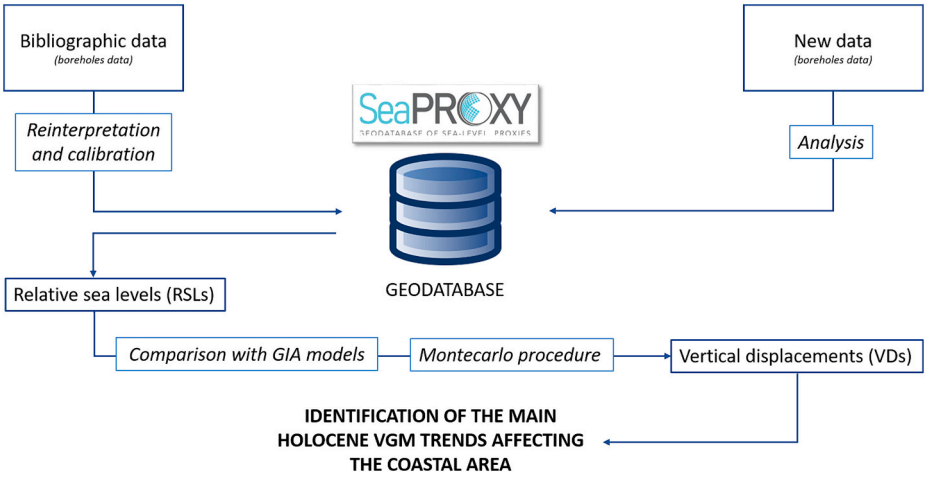

Fig. 2. Workflow of the methodological approach used in this research.

et al., 2016a), the GIA-modulated RSL changes deviate from the eustatic trend due to the sum of ocean syphoning and continental levering. The first stem from the migration of ocean water toward the subsiding peripheral forebulges that surround the former ice-sheets margins, while the latter result from the uplift of continents that are pushed upwards the subsiding ocean basins. The sum of the two results in a local RSL drop. Accordingly, a RSL highstand followed by a RSL drop between 8.0 and 5.0 ka BP are expected in the Cadiz Bay area, which has directly impacted the coastal evolution.

In this study, we aim to reconstruct the Holocene geomorphological evolution of the Bay of Cádiz and its relationship with relative sea-level changes and associated vertical displacements. We apply a multi-proxy approach that integrates indirect surveys, onsite observations, sediment coring and radiocarbon dating of samples, and reconstruction of RSL changes through high precision sea-level markers. The main objectives are (i) to calculate a Holocene RSL curve by applying a statistical approach, and (ii) to generate a new set of GIA models based on field data according to different ice-sheet chronologies (Peltier, 2004: De Boer et al., 2014; Peltier et al., 2015). For this purpose different types of stratigraphic sea-level markers have been considered, derived from new data and reinterpretation of bibliographic sources.

2. Geological and archaeological setting

The northern bay of Cádiz is characterized by the presence of a 30 km long and 15 km wide extensive littoral sedimentary plain located behind confining sandy barriers comprising beaches and dunes, which shelter a complex space with tidal flats and salt marshes, typical of a mesotidal coast (mean spring tidal range of 2.96 in the city of Cádiz; Benavente et al., 2007). The bay is positioned along low undulating hills modelled on Triassic and Neogene sedimentary materials (Fig. 1), as a consequence of the Plio-Pleistocene activation of strike-slip faults with a vertical component (Gracia et al., 2008). The tectonically subsided blocks recorded continuous coastal-marine flooding and sedimentary filling throughout the late Quaternary, reaching a thickness of up to 30 m at some points (Dabrio et al., 2000). During sea-level lowstands they acted as wide coastal plains traversed by the River Guadalete, plus other minor river courses (Gracia et al., 2010).

The outer, most external barrier is formed by a beach-dune system of 17 km of length running in a NNW-SSE direction, between the cities of Cádiz and San Fernando (Fig. 1). This results in a tombolo that links these two islands. After a small rocky headland, a second sandy barrier extends about 6 km to the south. These sandy barriers rest on previous Quaternary deposits formed by a series of marine terraces of Lower to Upper Pleistocene age (González-Acebrón et al., 2016). About one mile from this coast to the west a similar rocky shoal developed parallel to the coastline, forming a submerged platform structurally controlled, between 6 and 1 m below low-tide level (Fig. 1).

Between Puerto de Santa María and Puerto Real cities (Fig. 1) the bay is formed by another sand barrier, in this case N-S oriented (the Valdelagrana spit-barrier, 7 km long) and a wide extension of salt marshes in the sheltered zone. The salt marshes were comprehensively transformed for salt harvesting during historical times and artificially drained and desiccated in the 1950s. The marshes feature two main drainage channels: the Guadalete River, one of the most important rivers in Southern Spain, and the "river" San Pedro, a former course of the Guadalete River which now only acts as a tidal channel after its artificial disconnection from the main fluvial channel in the eighteenth century (Martínez-Sánchez et al., 2023). The present mouth of the River Guadalete, located in the town of Puerto de Santa María, is an artificial channel initially excavated for navigation purposes by the Romans 2000 years ago (Gracia et al., 2008).

The Valdelagrana spit-barrier shows a distinctive log-spiral shape, associated with the Guadalete river mouth and the dominant southward coastal drift. Positioned near the River Guadalete and open to the Atlantic Ocean's waves, this area has seen the formation of a complex late Holocene beach ridge system. >20 ridges have been identified by Rodríguez Polo et al. (2009) and categorized into three primary phases by Dabrio et al. (2000). These ridges have respectively developed with a parallel orientation during the succession of each phase. Over the years, multiple researchers have deeply studied this sedimentary environment, dealing with geomorphological mapping and age determination through radiocarbon techniques (Dabrio et al., 2000; Alonso et al., 2015, among others).

The city of San Fernando occupies an elevated landform of diapiric origin. The diapiric processes began in the Late Pleistocene, influencing Triassic clay and gypsum formations and leading to the formation of a hill that stands 40 m above the neighbouring tidal areas and marshlands, with movements still active today (Gracia et al., 2008). The southern bay, lying south and southeast of San Fernando island, is protected from the ocean by an outer barrier. This region embodies a broad NNE-SSW valley that traces back to river activities (Mediavilla et al., 2004; Gracia et al., 2010), marked by the presence of vegetated salt marshes. Historically, these marshes were converted into salt pans, a practice that started before the Roman era and persisted until the mid-1800s (Gracia et al., 2017). Today, many of these salt pans lie deserted and have been drained by the Sancti Petri tidal channel, with the region receiving water from various small river streams.

As well as coastal plains and estuarine regions in general (Allen, 2000), the Bay of Cádiz has been characterized by human occupation since historical times despite the exceptional dynamism of the area related to the interplay between marine phenomena like tides and

Fig. 3. Location of the boreholes considered in the present work.

currents and river-related aspects like floods. In general, the primary processes characterizing this type of coastal environments is sedimentation, with accretion being predominant (Alberico et al., 2012; Rahman and Plater, 2014; Aranda et al., 2020). Moreover, shifts in relative sea levels have transformed the regions influenced by these phenomena (Edwards and Horton, 2000; Pappone et al., 2012; Sampath et al., 2015; Bozi et al., 2021), compelling human societies to adjust to the evolving landscape (Fa et al., 2000; Mattei et al., 2019; Bailey et al., 2020). It's believed that Phoenicians settled in the Bay between 1100 and 800 BCE, making Cádiz one of the most ancient cities in Western Europe (Niveau de Villedary and Ruiz Mata, 1995). Notably, within the Bay of Cádiz lies the Phoenician settlement of Doña Blanca. Located on the northern edge of the Guadalete River estuarine sediment plain, this settlement is renowned in southern Iberia. Historical records show that this area has been impacted by sea-level fluctuations and has seen significant sedimentary infilling, with over 30 m of salt marsh deposits recorded during the Holocene (Dabrio et al., 2000).

In the last thousand years, this location has been a preferential site for the settlement of different human groups, forming communities that knew navigation techniques (Niveau de Villedary and Ruiz Mata, 1995). The survival of these groups was achieved through the exploitation of both marine (fisheries, salt harvesting) and terrestrial resources, available in the fertile low fluvial basin of the Guadalete River, close to the fluvial valley of the rich Guadalquivir River (Gracia et al., 2017). Over time, the strong connection between the local population and the river valleys near the coast has been fostered by maritime commercial

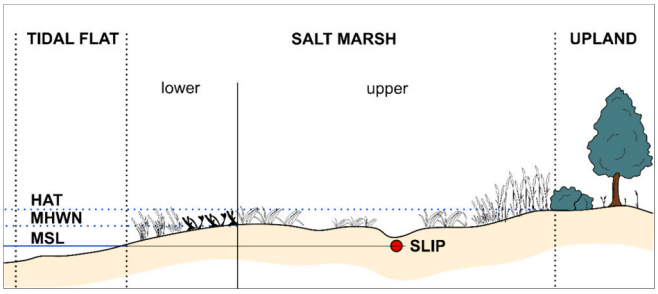

Fig. 4. Stratigraphic deposits within a salt marsh environment (MSL: mean sea level; MHWN: mean high water neaps: HAT: highest astronomical tide).

Table 1
Description of the stratigraphy of borehole S10, performed in the area of La Carraca. Contacts between units are largely conformable, typical of a prevailing aggradational environments.

Cores	Sedimentary Units	Thickness (m)	Lithofacies	Environmental Interpretation
S10	V1	1.00	Brown muddy sand with centimetric and millimetric (~3–15 mm) crystalline calcareous clasts.	Desiccated salt marsh
	U3	12.80	Dark grey mud with angular macro-clasts within the first centimeters.	Salt marsh
			Dark grey mud with remains of whole shells and gastropods	Salt marsh
			Dark grey mud with centimetric crystalline calcareous clasts.	Salt marsh
			Grey mud with scattered bioclasts	Salt marsh
	F	2.20	Coarse-grained sands with abundant remains of shells and millimetric rounded clasts.	Continental/ fluvial environment
			Yellow muddy sand.	Continental/ fluvial environment

activities (Alonso et al., 2009).

3. Methods

In this study, we implemented a workflow with the aim of evaluating a dataset comprising bibliographic and unpublished stratigraphic Holocene RSL data. The compiled data were then compared to three local GIA models produced specifically for the study area. This comparative approach aimed to unravel the varying factors influencing sea-level changes, ultimately determining the vertical land shifts and associated coastal trends impacting the Bay of Cádiz over the past 7.0 ka. A comprehensive overview of the methodologies employed, detailed in subsequent sub-sections, can be found in Fig. 2.

3.1. Stratigraphic and sedimentological analysis and dating

The stratigraphic dataset is composed of 19 boreholes that were collected in the area (Dabrio et al., 2000; Arteaga et al., 2008; Gutiérrez-Mas, 2011; Alonso et al., 2015; Salomon et al., 2020; Caporizzo et al., 2021), which were reinterpreted and combined with unpublished data derived from 3 new cores (Fig. 3). The new stratigraphic dataset is represented by a total of 36 m sediment thickness, recovered from three mechanical boreholes located within the Southern Bay of Cadiz (Gracia and Martín, 2009).

The new boreholes reached depths between 5 and 23 m. The continuous cores were stored in appropriate coring boxes and kept at the laboratories of the University of Cádiz. The description of the stratigraphic succession was carried out in three different stages: i) initial visual description of the sediments (type, colour, presence of organic remains and organisms); ii) detailed analysis of the sand fractions, separated by sieving, using a stereomicroscope; iii) analysis of the clay fraction on a petrographic microscope.

The sediment cores were classified based on the different lithofacies and sedimentary units identified in their sequences for which the inference of the different depositional environments was crucial to understanding the Holocene stratigraphy and tracing the paleo-coastline position. Data were processed in a GIS environment (ArcMap10.4) by using as basemap the DTM (5 × 5 m) from the Spanish National Geographical Institute available online.

Several organic samples, mainly constituted by shells in living positions recovered along the stratigraphic succession, were directly dated through the use of the radiocarbon dating technique by commercial Beta Analytic™ laboratories. The samples were differentiated according to their $\delta^{13}C$ value and calibrated using Calib 8.20 (http://calib.org/calib) software (Stuiver et al., 2021). The IntCal20 and MARINE20 calibration curves, with a 2σ range, were adopted for terrestrial and marine fractions, respectively.

In order to compensate for the reservoir effect of marine radiocarbon (ΔR), a weighted ΔR of −108 ± 31 14C years was adopted (Martins and Soares, 2013). In the present work, radiocarbon dates are reported in cal ka BP, i.e. calibrated kilo annum before present (1950 CE). The recalibration procedure and correction were applied to all the bibliographic radiocarbon dates, in order to allow comparison among the different chronological data.

3.2. RSL data and curve

The reinterpretation of pre-existing published data was combined with new measurements in a standardized geodatabase in order to produce a new suite of Holocene sea-level data using a wide range of proxies and following the most recent scientific protocols (Hijma et al., 2015; Khan et al., 2019). Most part of the database is composed of precise measurements of the former sea level (sea-level index points - SLIP, i.e., a point that constrains the sea level in space and time, Shennan et al., 2015), even if a part of it was populated with marine (MLPs) and terrestrial limiting points (TLPs). To qualify as an SLIP, several criteria must be assessed: the indicator's location and age, and its elevation. This assessment requires consideration of the vertical correction in relation to the indicative meaning (IM, i.e. established correlation between the marker and the Mean Sea Level (MSL); Shennan et al., 2015). The indicative meaning comprises two elements: i) the Indicative Range (IR), which denotes the elevation span wherein the marker is formed, and ii) the Reference Water Level (RWL), representing the central point of the previously mentioned span (Shennan et al., 2015).

The sea-level geodatabase, sourced from stratigraphic measurements, aligns with the methodologies recently established for the Mediterranean region (Rovere et al., 2016b; Vacchi et al., 2016) and extensively adopted in contemporary research (for instance, Brisset et al., 2018; Stocchi et al., 2018; Karkani et al., 2019). For SLIPs, the value for each dated specimen ($SLIP_n$) is computed using the formula from Shennan and Horton (2002):

$$SLIP_n = A_n - RWL_n \quad (1)$$

In this equation, A_n represents the proxy altitude, and RWL_n is the proxy's reference water level.

If samples did not have a direct association with a previous RSL, terrestrial (TLP) or marine (MLP) limiting points were assessed, as

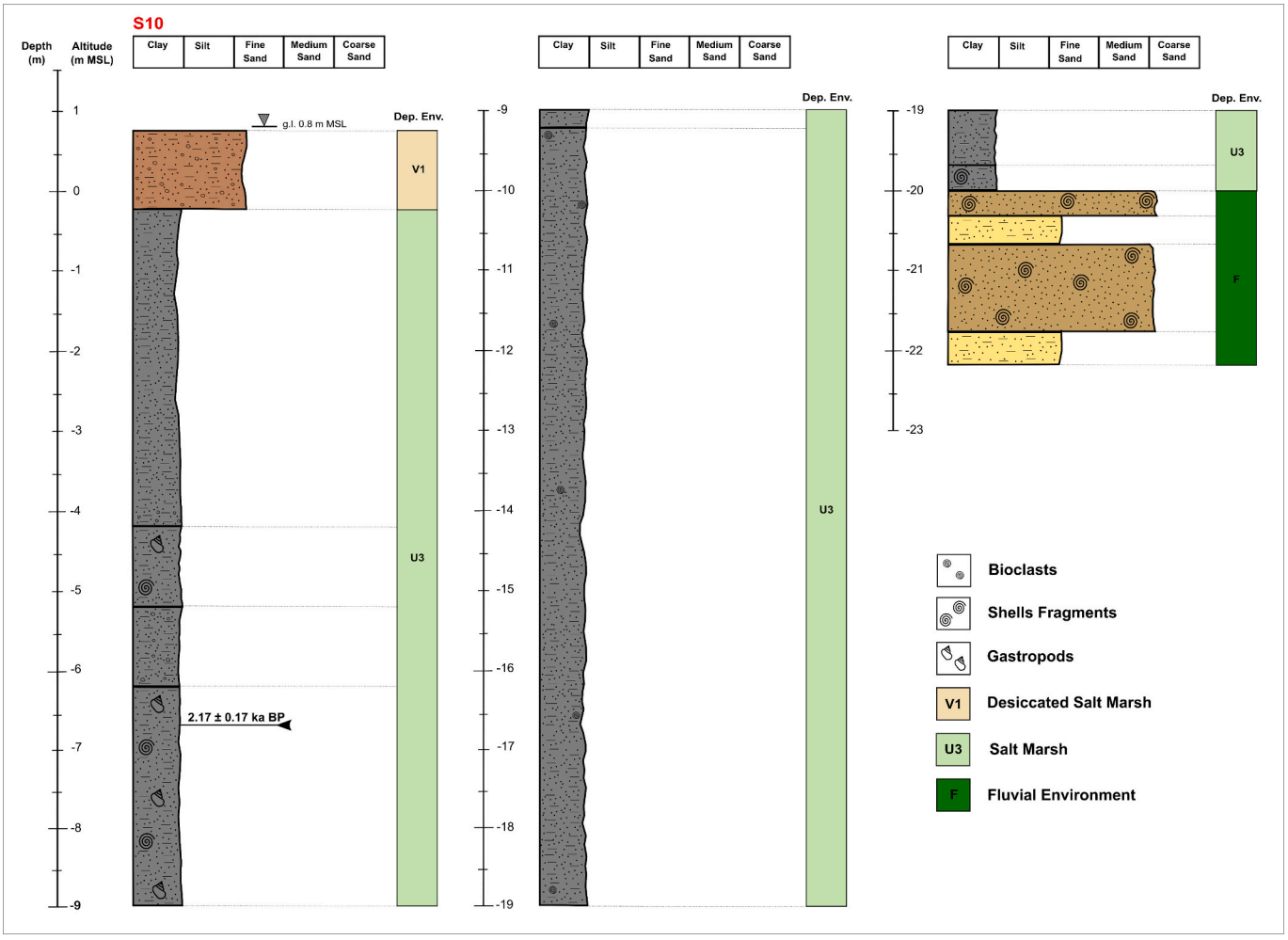

Fig. 5. Schematic stratigraphic logs of the new drilling S10 carried out in La Carranca area (for location see Fig. 3).

delineated by Shennan et al. (2015). TLPs, like dunes and backshore deposits, and MLPs, such as shoreface deposits, restrict the prior MSL either above or below a reference point during their formation.

As outlined by Vacchi et al. (2016), salt marshes are typically found near vast deltas and coastal lagoons. Their samples can serve as SLIPs by determining their IM (Shennan et al., 2015). We assume for this kind of sample an Indicative Range (IR) ranging from the HAT (i.e. elevation of the highest predicted astronomical tide, Shennan et al., 2015) to the MSL (i.e. arithmetic mean of hourly heights observed, Shennan et al., 2015; Vacchi et al., 2016) and an RWL equal to half of the IR (Fig. 4):

$$\mathrm{SLIP}_{\text{salt marsh}} = \mathrm{A} - \frac{\mathrm{HAT} - \mathrm{MSL}}{2} \quad (2)$$

The most precise data of the collected database allowed calculating the RSL curve for the last 12.0 ka by applying the Errors in Variables Integrated Gaussian Process (EIV IGP) Model, which performs the Bayesian inference on historical rates of sea-level change (Cahill et al., 2015). The EIV IGP model, providing the mean of the likelihood for the observed data, captures the continuous and dynamic evolution of sea-level change with full consideration of all available sources of uncertainty.

3.3. GIA models and Monte Carlo simulation

The GIA processes are commonly described by the sea-level equation (SLE), an integral equation that allows for the computation of relative sea-level changes that are driven by the mass variation of the continental ice sheets and modulated by the response of the Earth's mantle (Farrell and Clark, 1976; Milne and Mitrovica, 2008; Spada and Stocchi, 2007).

In this research, the SLE has been solved employing three ice sheet chronologies (i.e. ICE-5 G from Peltier, 2004; ICE-6 G from Peltier et al., 2015; ANICE-SELEN coupled ice-sheet - sea-level model from De Boer et al., 2013, 2014), which describe different melting histories since the Last Glacial Maximum (LGM; 21 ka BP) and equivalent sea level (ESL).

For the creation of the GIA models referred to the study area, the SLE has been solved by combining the forementioned ice-sheet chronologies and solid Earth rheological models where the solid Earth is assumed to be spherically symmetric, self-gravitating, rotating, radially stratified and characterized by linear Maxwell viscoelastic layers. A suite of 54 RSL curves was produced for the Bay of Cádiz assuming three values of lithosphere thickness, respectively of 60 km, 90 km and 120 km, and considering values for the viscosity of the lower and intermediate mantle ranging between 2 and 10, 0.5–1 and 0.2–0.5 Pas, respectively.

Then, to reconstruct the local RSL history and consequently discern between the GIA-driven RSL changes and the RSL variations related to the local VGMs, the obtained RSLs were compared with the GIA models.

For each sea-level marker, all potential Vertical Displacement (VD) values were computed using a Python 3.7 script leveraging a Bayesian Statistical method based on Monte Carlo simulations (following the methodology firstly applied in Mattei et al., 2022), a renowned statistical sampling method widely applied across various scientific disciplines (Eckhardt, 1987).

Specifically, given each RSL value and related uncertainties, the Monte Carlo process generates a set of '*n*' possible random VD values

Table 2
Description of the stratigraphy of the boreholes performed within the salt marsh of Chiclana de la Frontera (S12, and S15). Contacts between units are basically depositional, typical of a prevailing aggradational environments.

Cores	Sedimentary Units	Thickness (m)	Lithofacies	Environmental Interpretation
S12	V1	2.30	Dark brown mud. Coarsening upward sequence from 200-cm deep	Desiccated saltmarsh
	U3	2.70	Dark grey mud with finer grain size than the facies located above and isolated intercalation of small-size bioclasts levels.	Salt marsh
S15	V1	1.00	Present-day soil with remains of roots.	Desiccated saltmarsh Present-day soil
	U2	0.40	Yellow muddy sand with clasts and roots remains.	High-energy event
	U3	5.40	Black and dark grey mud with the presence of gastropods and macrofauna remains (shells).	Salt marsh
			Dark grey mud with some shells remains at the base.	Salt marsh
	U4	0.50	Dark grey mud.	Intertidal environment Tidal channel
	U5	0.70	Yellowish light grey sandy mud with clasts. Presence of a block of Roca Ostionera Formation at the base marking the beginning of the recent sedimentary sequence.	Marine Environment

algorithmically derived by computing the difference between observed (RSL_O) and predicted (RSL_P) sea-level positions from the GIA models:

$$VD_n = RSL_{On} - RSL_{Pn} \quad (3)$$

Here, '*n*' is set to 1000.

The Python routine displays the distribution of VD values on a histogram, where the peak represents the most probable value. Then, in order to extract the final VD, strongly influenced by the values of the peak but mitigated by the others, the average value is determined among the 1000 computed before together with the related uncertainty.

Together with the determination of local Vertical Ground Movements (VGMs), the associated subsidence or uplift rates (R_V) were also deduced using the Python 3.7 script. This is achieved by dividing the 'n' random VD values by the age of the proxy (T):

$$R_V = \frac{VD_n}{T} \quad (4)$$

Employing this statistical method in reconstructing sea-level history (Stanford et al., 2011) significantly minimizes errors associated with quantifying local VGMs. This is achieved by randomly generating a vast array of potential VD values within a specified range.

3.4. Geodatabase

The compiled RSL geo-database was housed in a specialized web-GIS platform named SeaProxy, accessible at (http://dist.altervista.org/seaproxy/). The utilized database is an open-source RDBMS (Relational Database Management System) supported by Oracle, known as MySQL. This platform offers a robust solution for web-based applications that handle vast volumes of interrelated data. SeaProxy was designed with a dual intention: to enable seamless remote collaboration among different research groups and to serve as a freely accessible tool for scientists interested in sea-level research.

The SeaProxy database is organized into four primary sections:

Section A: containing ID and bibliographical references.

Section B: featuring geographic location details.

Section C: showing information on dating techniques, encompassing the horizontal positioning of RSL and its associated uncertainties.

Section D: Encompassing various details like the method of measurement, including the sampling approach, stratigraphic data, GPS setup, tidal fluctuations, specimen elevation, Indicative Meaning, and inferred RSLs alongside their uncertainties.

4. Results

4.1. Boreholes description

The sedimentological analysis performed on the core logs led to the identification of six distinct sedimentary units, associated with those identified within the Northern Bay in Caporizzo et al. (2021), referred to as desiccated salt marsh (V1), high-energy deposit (U2), salt marsh (U3), and tidal (U4), shallow marine (U5) and fluvial (F) environments.

Between these units, the interpretation of U3 as salt marsh is focal as four samples were picked and radiocarbon-dated from this unit detected in all the three newly collected cores, to update the RSL database for the Bay of Cadiz (see section 4.2). In S3, where the unit is perfectly preserved, four facies are distinguishable:

- Dark grey mud with angular macro-clasts within the first centimeters;
- Dark grey mud with remains of whole shells and gastropods;
- Dark grey mud with centimetric crystalline calcareous clasts;
- Grey mud with scattered bioclasts.

The interpretation as salt marsh environments is based on the regional knowledge and previous works like the one by Alonso et al. (2015), where the same facies mostly constituted by clays, with a high content of organic matter, was explained as a typical salt marsh deposit in the Northern Bay. Another evidence supporting the interpretation is the sedimentation rate calculated in S3 (0.3 mm/y), perfectly matching previous works from salt marsh deposits in the area (Morales et al., 2003). Finally, a possible lacustrine origin for these clay deposits can be discarded according to previous works carried out in the Gulf of Cadiz and its surroundings (Boski et al., 2002; Teixeira et al., 2005; Sampath et al., 2015; Rodríguez-Ramírez et al., 2016; Cáceres et al., 2018; López-Sáez et al., 2018; Sousa et al., 2019), by which the prevailing mesotidal regime prevents from closing the outer barriers to form closed lagoons in favour of the establishment of semi-closed salt marshes.

The cores are located in two different sectors within the Southern Bay of Cádiz, the area of La Carraca (core S10) and the salt marshes (S12 and S15) of Chiclana de la Frontera (see Figs. 1 and 3 for location).

- La Carraca (S10)

Borehole S10 is located within the municipality of San Fernando in the area of La Carraca, occupied by several military settlements and shipyards. The core has a length of 23 m and it is the deepest among all the drilling performed by Gracia and Martín (2009).

Within the stratigraphic succession, seven different lithofacies were identified and distributed in three sedimentary units (Table 1 and Fig. 5). While the upper unit V1 is mainly constituted by muddy sands with no fossil content, the salt marsh environment identified by unit U3 is made of dark mud with significant traces of macrofauna, and the coarse-grained sands of unit F represent a continental environment,

Fig. 6. Schematic stratigraphic logs of the new drillings S12 and S15 carried out in the Southern Bay of Cádiz (for location see Fig. 3).

most likely fluvial.

Two samples were collected within U3 for radiocarbon dating, at a depth of 7.5 and 20.08 m, exhibiting a calibrated age of 2.17 ± 0.17 ka BP and 6.99 ± 0.20 ka BP, respectively.

- Salt Marsh of Chiclana de la Frontera

Within the salt marsh of Chiclana de la Frontera two different cores were carried out in a NW-SE direction.

Core S12, with 5 m depth, is located along the eastern bank of Sancti Petri tidal channel. In its stratigraphic succession, two lithofacies were detected and assigned to sedimentary units V1 and U3 (Table 2 and Fig. 6). While the upper dark unit identifies a desiccated salt marsh environment, the finer-grain mud below was linked to an active salt marsh system. At a depth of 4 m, a shell sample was collected within U3 for radiocarbon dating exhibiting a calibrated age of 2.12 ± 0.18 ka BP.

Core S15 is located west of the Sancti Petri tidal channel, close to the city of San Fernando. Along this borehole with a depth of 8 m, six lithofacies were identified and related to 5 different sedimentary units (Table 2 and Fig. 6). Starting from the top, the soil rich in roots identifying the desiccated salt marsh environment is separated from the dark mud rich in macrofauna of the salt marsh by a thin layer of yellow sands probably related to a high-energy event, very likely a tsunami event (See Gracia et al., 2022, for details about historical tsunamis recorded in the Bay of Cádiz). Below, the deeper sandy mud of U5 testifies the transition from a marine environment to a more restricted tidal system represented by the dark mud of U4.

Two samples were collected within U3 for radiocarbon dating, at a depth of 3.8 and 5.5 m, exhibiting a calibrated age of 2.65 ± 0.19 ka BP and 2.97 ± 0.19 ka BP, respectively.

4.2. Sea-level data

A total of 35 sea-level markers were collected in this research, which 14 were classified as SLIPs, 11 as MLPs and 10 as TLPs. While the data regarding the Southern Bay are mainly derived from the new and unpublished stratigraphic columns described in the precedent section, the SLMs identified in the Northern sector were extracted from previous works published between 2000 and 2021. In particular, 4 SLIPs were extracted from the new boreholes (S10, S12, and S15), 3 SLIPs, 10 TLPs and 3 MLPs from Dabrio et al. (2000), 1 MLP from Arteaga et al. (2008); 3 MLPs from Gutiérrez-Mas (2011), 3 SLIPs from Alonso et al. (2015); 3 MLPs from Bernal-Casasola et al. (2020), and 4 SLIPs and 1 MLP from Caporizzo et al. (2021) (Fig. 7).

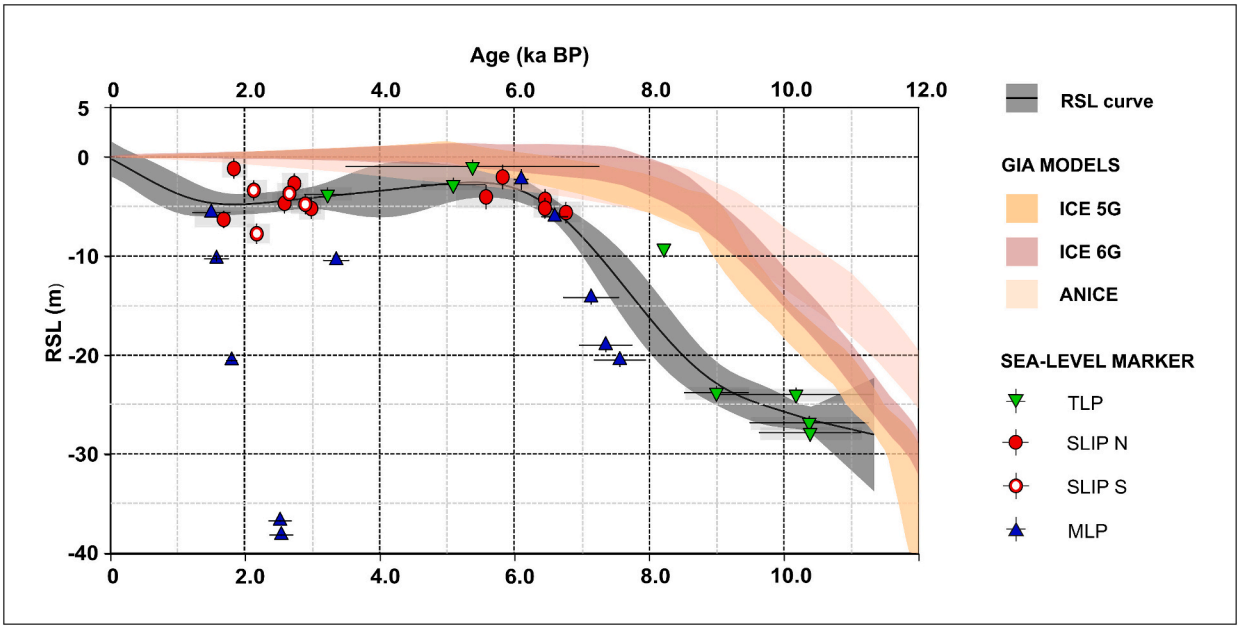

Fig. 7. Comparison between the RSL curve calculated by using the EIV IGP Model by Cahill et al. (2015) from the most precise RSL data collected in our geodatabase (squared in grey), and GIA models for the Bay of Cádiz during the Holocene. Location of SLIPs (red circles) within the Bay of Cádiz: northern sector, solid circles; southern sector, void circles. (For interpretation of the references to colour in this figure legend, the reader is referred to the web version of this article.)

In the Northern sector, the 7 new SLIPs are related to salt marsh deposits dated between 6.45 ± 0.179 cal. ka BP and 2.58 ± 0.198 cal. ka BP, while the others were deduced from the re-interpretation of intertidal deposits from Dabrio et al. (2000), dated between 5.86 ± 0.428 cal. ka BP and 1.67 ± 0.445 cal. ka BP. TLPs were mainly obtained by plant debris and shells in floodplain deposits dated between 10.38 ± 0.754 and 3.220 ± 0.342 cal. ka BP. The 7 marine deposits (MLPs) covered a period between 7.13 ± 0.409 and 1.49 ± 0.276 cal. ka BP. The general rising trend of this dataset was decisively positioned under the GIA models during the early Holocene up to 6.0 ka BP when some SLIPs and TLP are positioned in the lower part of our glacio-hydro- isostatic signal (Fig. 7). MLPSs are represented by the sedimentary infilling of a palaeogorge that crossed the city of Cádiz originally excavated by the River Guadalete. The relict palaeochannel was already mentioned by ancient texts from Strabo and Pliny (Corzo, 1980; Ponce Cordones, 1985) and its genesis can be ascribable to late Pleistocene Age, during the sea level lowstand related to the last glaciation (Llave et al., 1999; Alonso et al., 2009; Gracia and Alonso, 2009).

The RSL rise in the Northern sector is testified by salt marsh deposits (4 SLPs) and marine sediments (1 MLP) dated between 1.79 ± 0.76 and 6.09 ± 0.10 cal. ka BP and positioned several meters under the GIA models calculated in this research (Fig. 7).

The RSL curve deduced from our dataset indicates a rising trend up to 5.8 ka BP, when RSL reached a position very close to the present one, and a subsequent slight fall during the Iron Age (about 2.8 ka BP). After that, a new input of RSL rise brought the sea level to the present one.

4.3. GIA models and VD

In accordance with the methodology described in section 3.3, using the ICE-5 G (Peltier, 2004), ICE-6 G (Peltier et al., 2015), and ANICE-SELEN ice-sheet models (De Boer et al., 2013, 2014), a set of 18 sea-level curves for the last 27.0 ka BP was computed for every ice-sheet chronology combining together the different values of mantle viscosity and lithosphere thickness. The results are shown in Fig. 8 (8a: ICE-5 G; 8b: ICE-6 G; 8c: ANICE-SELEN).

It is possible to observe that in the simulations carried out using ICE-5 G and ICE-6 G models (Figs. 8a and b), the GIA-driven RSL variations show a slight increase of the RSL between 8.0 and 2.0 ka BP that exceeds the current values. In particular, the ICE-5 G (Peltier, 2004) set of RSL curves shows a local RSL rise starting around 6.5 ka BP with a maximum peak of about 1.5 m MSL around 5.0 ka BP. On the other hand, the RSL curves carried out using the ICE-6 G chronology (Peltier et al., 2015) exhibit a similar RSL rising trend but starting at 8.0 ka BP and with a peak of about 1.0 m MSL around 5.0 ka BP.

New sea-level data were obtained both by reinterpreting the bibliographic sources and analyzing new boreholes. Among them, the high-precision SLIPs were compared with the GIA model produced for the study area in order to evaluate the related VD-rates that occurred over the last 7.0 ka. The obtained results are synthesized in Table 3.

5. Discussion

5.1. GIA and VD outputs

The first result of this study was a new set of GIA models describing the expected isostatic response to climatic and/or eustatic forcing during the Holocene in a far field area. The models highlight a Late Holocene high-stand and a related sea-level drop attributable to the two-fold action of two phenomena related to the interglacial dynamics: the ocean syphoning and the continental levering (Clark et al., 1978; Khan et al., 2015; Rovere et al., 2016a; Stocchi et al., 2018). Indeed, after the Holocene high-stand about 5.0–7.0 ka BP, a slowdown in the water release within the oceanic basins related to the ice-sheets melting occurred, leading to the collapse of the nearfield forebulges. Consequently, the latter started to draw water toward them producing a RSL drop along the continental far-field margins (i.e. ocean syphoning). At the same time, since the LGM, the oceanic basins were loaded with an increasing water weight which firstly produced local subsidence and, then a related uplift along the coastal sectors of the continental far-field margins, in order to compensate for the lithospheric movements (i.e. continental levering).

5.2. Subsidence and sediment compaction

The second major result was the evaluation of the coastal subsidence affecting the Bay of Cadiz during the Holocene by comparing the RSL

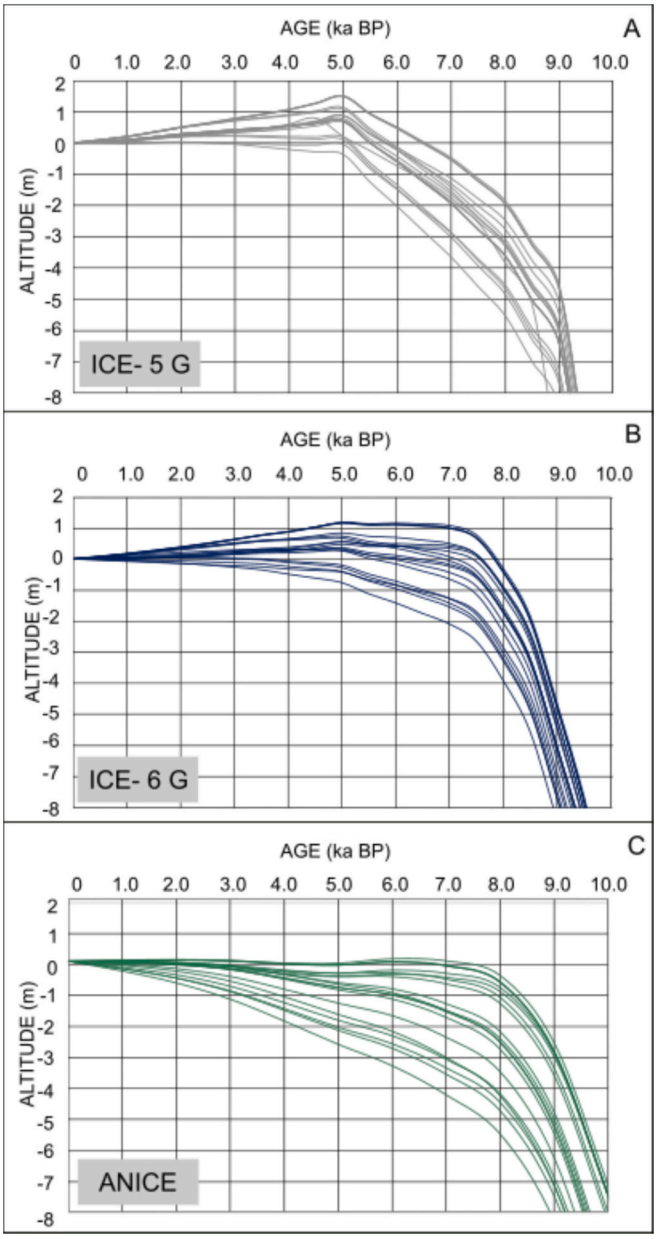

Fig. 8. RSL curves obtained using the ice-sheet chronologies ICE-5 G by Peltier, 2004 (grey curves, box A), ICE-6 G by Peltier et al., 2015 (blue curves, box B), and the ANICE-SELEN coupled ice-sheets - sea-level model by De Boer et al., 2014 (green curves, box C) coupled with a solid Earth rheological model that supposes 6 values for the lower and intermediate mantle viscosity ranging between 2 and 10, 0.5–1 and 0.2–0.5 Pas and three values of lithosphere thickness of 60 km, 90 km, and 120 km. (For interpretation of the references to colour in this figure legend, the reader is referred to the web version of this article.)

database and specific GIA models (Supplementary material 3). Indeed, regarding the precision of the new RSL data coming from the stratigraphic analysis, even if the absence of a detailed palaeoecological analysis prevented from reconstructing the Holocene paleoenvironmental evolution of the salt marsh, the radiocarbon dating of this unit at different altitudes provided new robust information regarding the Holocene RSL changes in the Bay.

Even if other authors discard any significant sediment compaction during recent, Holocene, times (Boski et al., 2008; Delgado et al., 2012) due to the virtual absence of peat in other borehole records previously made along different salt marshes of this region, subsidence can be also related to silts and affect sea-level reconstructions in coastal marshes (Finkelstein and Ferland, 1987; Shennan, 2003). Consequently, in the present work an approximation to the possible influence of land subsidence and sediment compaction was made comparing the RSL records and the geophysical predictions.

This comparison was carried out through a statistical procedure that allowed obtaining a robust evaluation of the local coastal subsidence due to sediment compaction (van Asselen et al., 2017, 2018). The new database of RSL data significantly improved the previous knowledge regarding the Holocene RSL trend of this peculiar key far-field area where a regional mid-Holocene highstand was expected according to the GIA models for the same latitude.

The applied methodology allowed the precise evaluation of the vertical and spatial distribution of the Mid-Holocene coastal subsidence characterized by a slight differential behavior detected between the Northern Bay, for which the recent evolution was mainly driven by the sedimentary infilling from the Guadalete River, and the southern sector, where the evolution was linked to the dynamics of the main tidal channels and related tidal, and in which the subsidence could be related also to the thickness of the fine deposits. Fig. 9 shows the Age - Depth models obtained from data related to the same age (between 1.8 and 2.8 ka BP) located in both northern and southern bays. By analyzing the slope of the trendlines it was possible to assess that in terms of sedimentation rates, as well as in the case of the vertical displacements (Fig. 10) the two coastal sectors exhibited a broadly similar behavior. Moreover, the obtained values of the coefficient of correlation (R^2) are close to 1 (between about 0.92 and 0.94), indicating a good fit of the estimated trendline values to the actual data.

In particular, the subsidence rates of the Northern Bay are spread in two different orders according to the ages of the sea-level markers. The rates related to the boreholes performed more inland (PSM110, S8, and S7 in Table 3) and dated between 6.7 and 5.5 ka BP, are in perfect agreement and equal to −0.65 mm/yr. On the other hand, the subsiding rates characterizing the SLIPs of the more external cores (S1, S4, and S5 in Table 3), dated between 2.8 and 1.8 ka BP, exhibit values up to three times higher than the previous ones and a more pronounced variability moving northeast (ranging between −0.65 and − 2.66 mm/yr).

The difference in the rate values between the inner and outer cores is probably related to a different substratum (See Fig. 3 for location). While it is possible to assume that the stratigraphic succession of 110, S8, and S7 rest on an already consolidated substratum, the sedimentary sequences of cores S1, S4, and S5 should be located above a more recent fine and compactable material, which constitutes the latest, youngest infilling of the coastal plain. Lateral variations in the Quaternary sequence depth and the possible lateral variation of the proportion of silts and clays could have produced differential compaction and subsidence, influencing the final location of the dated levels. Since there is no information available regarding this point, we could not take it into account. This is one of the possible sources of uncertainty inherent to this methodology.

By comparing only the RSL-data coming from the more external boreholes, it is possible to observe that the subsiding rates of S4 are lower than those calculated from S1, S5, and 102 (Table 3 and Fig. 3). Taking into account the same age of the SLIPs, the reason can be related to different basal stratigraphic successions considering that the sequence of S4 covered older deposits constituted by coarser, sandy facies, presumably less compactable than the estuarine silts and clays located below S1, S5, and 102.

Concerning the subsiding rates resulting from the Southern sector, while the lowest values appear near the main tidal channel (S15 and S12 in Table 3 and Fig. 3), the highest value of 3.55 mm/yr (S10 in Table 3) is recorded in its northernmost area, the closest to the mainland of San Fernando city. This could be related to a higher rate of sedimentary aggradation, often higher in the high salt marshes. Additionally, borehole S15 shows an increase in sedimentary aggradation over time. These results are in accordance with present rates of salt marsh aggradation measured in the Southern Bay of Cádiz (Gracia et al., 2017).

Table 3
SLIPs identified in the northern (Dabrio et al., 2000; Alonso et al., 2015; Caporizzo et al., 2021) and southern (new data) sectors of the Bay of Cádiz with: sample ID (column 1); dated feature (column 2); conventional radiocarbon age (ka BP, column 3); calibrated radiocarbon age (cal. ka BP, column 4. See section 3.1 for calibration method) and related error (cal. ka BP, column 5); calculated RSL (m MSL, column 6) and related error (m MSL, column 7); calculated VD (mm/yr, column 8) and related error (mm/yr, column 9); source (column 10). For additional info regarding the radiocarbon dating see supplementary materials.

SLIP ID	Dated Feat.	Age	cal. Age	±2σ	RSL	±2σ	VD	±2σ	Source
PSM102_18	Shell	5.52 ± 0.21	5.81	±0.47	−2.00	±1.19	−0.24	±0.20	Dabrio et al., 2000
PSM110_2	Shell	5.30 ± 0.18	5.57	±0.45	−4.01	±1.19	−0.65	±0.27	Dabrio et al., 2000
S1_a2	Shell	2.89 ± 0.05	2.58	±0.19	−4.65	±0.98	−1.82	±0.40	Alonso et al., 2015
S4_a1	Shell	2.99 ± 0.04	2.74	±0.19	−2.65	±0.98	−0.98	±0.39	Alonso et al., 2015
S4_a2	Shell	2.27 ± 0.04	1.82	±0.18	−1.15	±0.98	−0.65	±0.55	Alonso et al., 2015
S5_a1	Shell	3.10 ± 0.07	2.88	±0.22	−4.79	±0.98	−2.66	±0.61	Caporizzo et al., 2021
S7_a1	Shell	6.09 ± 0.05	6.44	±0.18	−4.25	±0.98	−0.65	±0.23	Caporizzo et al., 2021
S8_a2	Shell	6.38 ± 0.05	6.75	±0.20	−5.59	±1.02	−0.65	±0.23	Caporizzo et al., 2021
S8_a3	Shell	6.09 ± 0.04	6.44	±0.17	−5.15	±0.98	−0.65	±0.23	Caporizzo et al., 2021
S10_a2	Shell	2.56 ± 0.03	2.17	±0.17	−7.75	±0.98	−3.55	±0.47	New data
S12_a1	Shell	2.50 ± 0.03	2.13	±0.18	−3.35	±0.98	−1.60	±0.48	New data
S15_a1	Shell	3.20 ± 0.03	2.97	±0.18	−5.35	±0.98	−0.48	±0.36	New data
S15_a2	Shell	2.94 ± 0.04	2.65	±0.19	−3.65	±0.98	−1.40	±0.39	New data

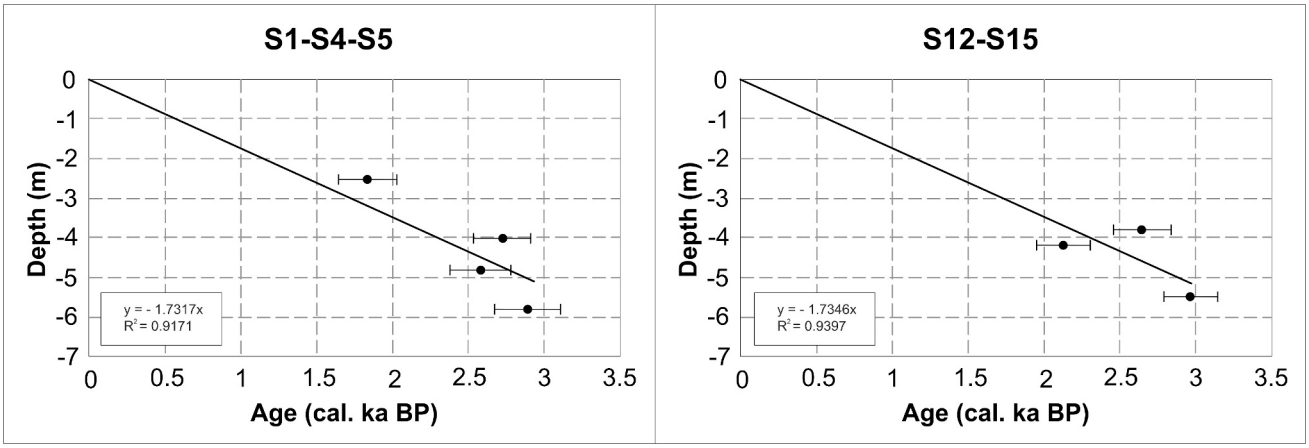

Fig. 9. Age-Depth models carried out from data related to the same age (between 1.8 and 2.8 ka BP) and located in northern (S1, S4, and S5 boreholes) and southern (S12, and S15 boreholes) bays. The coefficient of correlation R2 measures the trendline reliability. The obtained values of R2 are close to 1 (between 0.9171 and 0.9397), indicating a good fit of the estimated trend line values to the actual data.

Comparing all VD data together (Fig. 10), we can certainly assume that the whole area was affected by general subsidence, influencing the morphoevolution of the different zones with a variable entity and that the general trend appears to be homogeneous for both the main sectors of the Bay during the last 3.0 ka. Moreover, it is possible to observe that for the Northern Bay (solid circles in Fig. 9), which is the sector characterized by RSL data related to a wider time span, the SLIPs related to the last 3 ka are characterized by higher subsidence rates than the older ones. This can be most likely related to the highest compressibility of the younger sediments due to their higher primary porosity, a property that usually decreases with time in marsh sediments (Bahr et al., 2001). This interpretation is obviously dependent on the confirmation of such an assumption.

5.3. Regional correlation

From a regional point of view, a rapid postglacial sea-level rise is generally accepted for the Gulf of Cádiz, mainly based on the stratigraphic architecture of the continental shelf (Hernández-Molina et al., 1994; Lobo et al., 2001; Delgado et al., 2012; Carrión-Torrente et al., 2022) and on coastal geoarchives (Lario, 1996; Zazo et al., 2008). The rapid rise of sea level between 8.5 and 7.5 ka BP is interpreted as a result of the last melting phase of the Laurentide ice sheet (Turney and Brown, 2007). According to Goy et al. (1996) and Dabrio et al. (2000), about 6.0 ka BP sea level rising rate decelerated in the Bay of Cádiz, while following Boski et al. (2002), Teixeira et al. (2005) and Delgado et al. (2012), in the Algarve coast and Guadiana estuary (about 100 km to the west of the Bay of Cádiz) this deceleration took place earlier, about 7.5 ka BP. A similar sea level rising deceleration between 7.0 and 8.0 ka BP was detected by May et al. (2022) in the Western Mediterranean Spanish coast, near the Strait of Gibraltar. The results obtained in the present work are in clear accordance to those obtained by Dabrio et al. (2000) in the Bay of Cádiz. The reasons for this delay of about 1.5 ka between the rates recorded in Southern Portugal – Strait of Gibraltar and in the Bay of Cádiz are difficult to infer from the data exposed in the present work. Nevertheless, this does not exclude that additional geodynamic processes may play a significant role in the vertical variation of the Earth's crust. Among these, it would possible to consider mantle density anomalies related to the formation of atypical masses inside it (i.e, dynamic topography; Austermann et al., 2017; Rovere et al., 2023), by all means acting on much wider temporal and spatial scales. In any case, regardless of the specific causes, this deceleration favoured the beginning of sedimentary processes along the coast, firstly by filling the estuaries in the bays through aggradation, and afterwards, in the last 2.0 ka, by coastal progradation and tidal flat development due to climate forcing.

Hernández-Molina et al. (1994) and Lario (1996) considered that sea level reached a height equivalent to the present one or even higher around 7.0–5.0 ka BP, while other authors discard this possibility in the region, arguing that the sea level never reached the present height during the Holocene (Stanley, 1995; Boski et al., 2002; Leorri et al., 2012; García-Artola et al., 2018; May et al., 2022). In fact, markers of

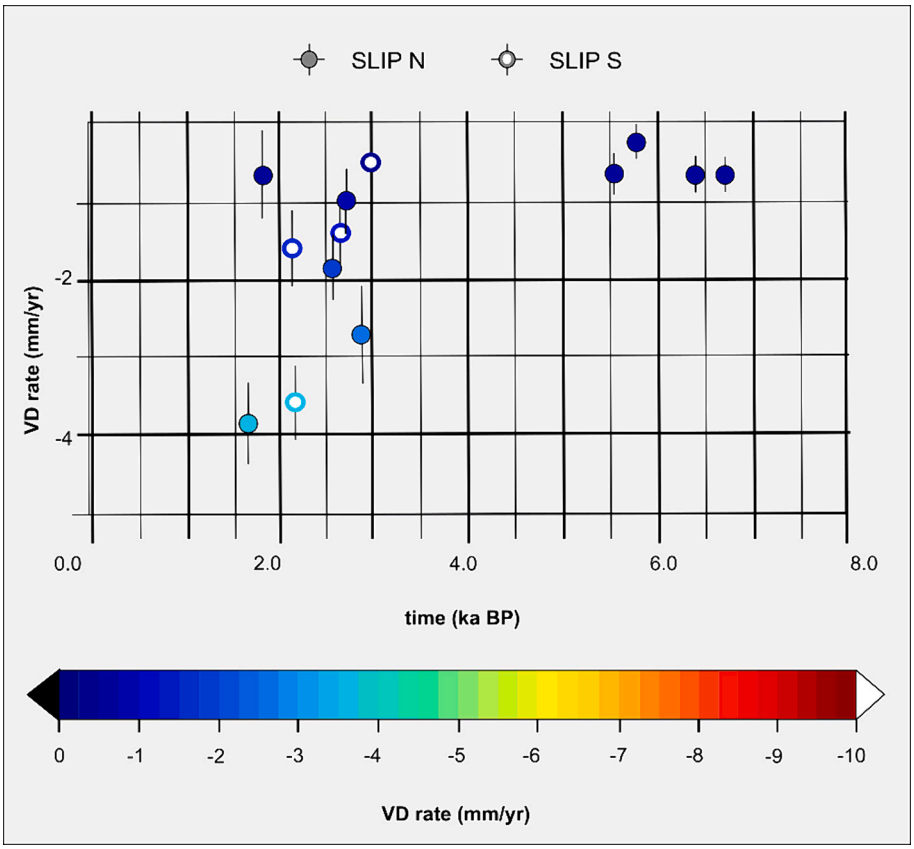

Fig. 10. Vertical displacement rates (mm/yr) measured through the Monte Carlo procedure in the Northern (solid circles) and Southern (void circles) sectors of the Bay of Cádiz.

Holocene sea levels above the present one are virtually absent in the Bay of Cádiz. South of Puerto Real, Gracia et al. (2000) identified a littoral deposit at 2.5–3 m above the present sea level, forming a marine terrace located in the inner border of the bay. Shell fragments from the deposit were sampled and dated by radiocarbon in 4.9–5.3 ka BP, although the dating was not corrected due to possible reservoir effect. The sedimentological nature of this deposit (a thin level of broken bioclasts without any inner structure) and the development of coastal research in the region during following years made the authors reinterpret this level as produced by an energetic wave event, very probably a tsunami, like the high energy event that hit this region between 5.7 and 5.3 ka BP (Gracia et al., 2022).

In a broad sense, the RSL curve obtained in the present work for the Bay of Cádiz is not far from those obtained in other nearby regions of Southern Europe (Khan et al., 2015; Vacchi et al., 2016) and confirms the hypothesis by which during the Holocene climatic optimum (about 6.5 ka) the sea level did not reach the present height, although it might have been close to it. According to the synthesis made by García-Artola et al. (2018) for the European Atlantic coasts, the Gulf of Cádiz, represented by records taken in the Southern Portuguese coast, is characterized by a rapid rise from −10.7 to −3.6 m in the period −8.5 to −7.2 ka, at a rate of 5.3 ± 0.6 mm/yr. In later times, these authors identify a series of index points indicating a significantly lower sea-level rising trend from −2.5 ± 0.5 m to +0.4 ± 0.9 m in the period −6.4 ka to −1 ka, at a rate of 0.5 + 0.2 mm/yr. These authors recognized a number of vertical uncertainties related to the indicative meaning of the samples, the determination of depths in cores, the elevation of the cores, tidal range, etc. It is worth to note that, following these authors, in the Algarve coast the only period where RSL virtually did not change was 3–2 ka BP, in accordance with other Southern European coasts. This regional sea-level relative stabilization coincides with the Iron Age period, when, according with the data presented in the present work, sea level in the Bay of Cádiz also stabilized or even slightly dropped. Nevertheless, with the existing data it is very difficult to establish accurate rates of sea level change in order to compare velocities at a regional scale.

For more recent times the method used in the present work hardly defines significant sea-level oscillations. Dabrio et al. (2000) related the generation of successive beach ridges in the Valdelagrana confining barrier (Fig. 1) to subtle sea-level oscillations during the late Holocene. Based on regional geoarchaeological and palaeoclimatic data, Losada et al. (2011) made a tentative sea-level evolution for the Spanish coast, by which three recent sea-level lowstands would have occurred: one in protohistoric times-Iron Age (3.0–2.5 ka BP), a second one during the barbarian invasions (1.5–1.2 ka BP) and the third one during the Little Ice Age (0.5–0.15 ka BP). According to these authors, high sea levels would have been attained during the Roman Epoch (2.2–1.8 ka BP), during the Medieval warm period (1.0–0.7 ka BP) and in the last century. However, these authors did not provide any numerical estimation of relative sea-level oscillation. In any case, local geoarchaeological data in the Bay of Cádiz (Alonso et al., 2009; Gracia et al., 2017) confirm the climatic evolution synthesized by these authors, and climate change could be considered as the main driver of all the subtle sea-level oscillations recently inferred for the region (Gracia et al., 2006).

5.4. *Palaeogeographical evolution*

The sediments studied in the present work were compared to those obtained and studied by other authors in nearby bays and estuarine environments: Teixeira et al. (2005) and Sousa et al. (2019) in the South Portuguese coast; Boski et al. (2002) and Sampath et al. (2015) in the Guadiana estuary; Cáceres et al. (2018) in the Huelva embayment, and

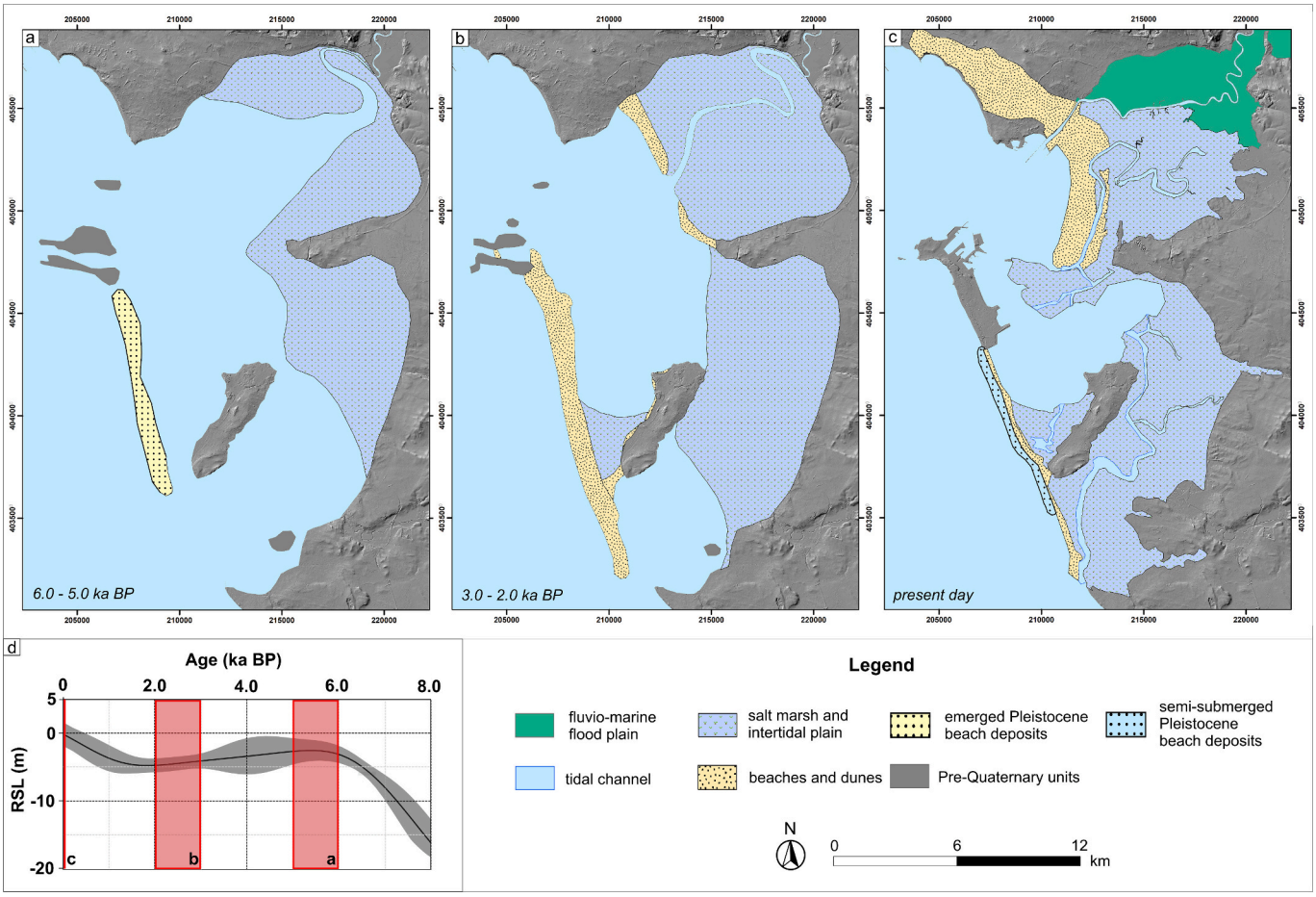

Fig. 11. Morpho-evolutive diagrams of the Bay of Cádiz for the last 6.0 ka. a: from 6.0 to 5.0 ka BP; b: from 3.0 to 2.0 ka BP; c: present-day; d: RSL curve produced for the study area highlighting the time spans represented in the vignettes.

Rodríguez-Ramírez et al. (2016) and López-Sáez et al. (2018) in Doñana estuary. Conclusions in all these works clearly indicate that all the bays and estuaries developed in this region evolved as salt marshes semi-closed by outer sand barriers, but always connected to the sea through permanently open inlets. The mesotidal regime prevailing along the Gulf of Cádiz prevents the closing of bays by sand barriers to form closed lagoons or coastal lakes, which are more typical of microtidal regimes, like the Mediterranean coast (Gómez et al., 2021).

The results obtained in the present work in terms of RSL change and recognition of depositional environments can be used for improving the palaeogeographical reconstruction and evolution of the Bay of Cádiz during the last 6.5 ka (Fig. 11), helping asses in broad terms the coastline position. In the last 20 years a number of studies have proposed different reconstructions of the Bay of Cádiz for the last millennia (Corzo, 1980; Alonso et al., 2004, 2009; Gracia and Alonso, 2009, among others). All of them considered that the last eustatic maximum, about 6.5 ka BP, reached a height slightly above the present one, and hence the Bay of Cádiz was considered as completely flooded. Only some isolated morphostructural relieves emerged as islands of different dimensions. However, the results obtained in the present work suggest that most probably sea level did not achieve such a height, which would have favoured the development of a certain sedimentary plain in the inner zones of the bay, composed by alluvial deposits (associated with the River Guadalete) and by incipient salt marshes (Fig. 11a).

Between the cities of Cádiz and San Fernando, several Pleistocene marine terraces and beachrocks lie around the present medium sea level. They were dated and studied in detail by González-Acebrón et al. (2016) and present a significant structural control. Given their locations, they necessarily would have outcropped above sea level between 6.0 and 5.0 ka BP. The Pleistocene beachrocks acted as firm substratum for the development of the present long tombolo and sand barrier existing between Cádiz and San Fernando that very probably reached its maximum extension around 3.0–2.5 ka BP, due to the episodic sea-level stabilization or slight drop (Fig. 11b). By that time and onwards, the development of the sand barriers promoted the expansion of salt marshes in the inner sheltered zones of the bay (Del Río et al., 2015). Very recently, the significant reduction of fluvial sediments supplied by the Guadalete River due to regulation works, together with other coastal engineering interventions, has produced severe erosion in Valdelagrana sand barrier and a rollover trend in the outer San Fernando beach barrier (Talavera et al., 2018). Although erosion in Valdelagrana has completely decreased, coastal retreat at Cádiz-San Fernando is still active (Fig. 11c).

This general proposal of palaeogeographical evolution is not far from those proposed by other authors for other estuaries and bay of the Gulf of Cádiz coast, like Algarve (Teixeira et al., 2005), Guadiana (Sampath et al., 2015) or Guadalquivir-Doñana (Rodríguez-Ramírez et al., 2019). Regarding the detailed drawing of the shoreline for different historical periods represented in Fig. 11, the successive maps have been elaborated by incorporating the most recent geoarchaeological findings and other reconstructions proposed by Arteaga et al. (2008), Alonso et al. (2009), Rodríguez Polo et al. (2009), Gracia et al. (2017), Caporizzo et al. (2021), and Martínez-Sánchez et al. (2023).

6. Conclusion

The main contribution of this study is represented by the integration

of previous and new knowledge regarding the RSL variations, both on regional and local scales, and the response of the coastal system to such modifications.

In the research, a precise evaluation of the coastal subsidence of the far-field area was carried out thanks to the assemblage of a robust dataset of RSL data obtained through the reinterpretation of bibliographic sources coupled with new stratigraphic data. The resulting geodatabase has been made available on an online platform (*https://dist.altervista.org/seaproxy/)* in order to be freely accessible.

Moreover, the local mid-Holocene response of the coastal system to the RSL variations was reconstructed both in terms of VDs and landscape evolution by differentiating between the northern sector of the bay, characterized by the presence of the Guadalete River, and the southern one, in which the tidally driven processes are responsible for the local coastal conformation. This is the first time that a Holocene RSL curve is obtained for the Spanish side of the Gulf of Cádiz and the resulting evolution is in accordance with other previous RSL reconstructions made in Southern Portugal. Differential trends detected between the northern and southern sectors of the Bay of Cádiz are subtle and interpreted as due to the different nature of the substratum upon which the studied sedimentary sections lie, leading to differential subsidence rates.

CRediT authorship contribution statement

C. Caporizzo: Writing – review & editing, Writing – original draft, Visualization, Validation, Software, Methodology, Investigation, Formal analysis, Data curation, Conceptualization. **F.J. Gracia:** Writing – original draft, Validation, Supervision, Resources, Project administration, Investigation, Formal analysis, Data curation, Conceptualization. **C. Martín-Puertas:** Investigation, Data curation. **G. Mattei:** Writing – review & editing, Writing – original draft, Visualization, Validation, Software, Methodology, Investigation, Formal analysis, Data curation, Conceptualization. **P. Stocchi:** Writing – review & editing, Writing – original draft, Validation, Methodology, Formal analysis, Data curation, Conceptualization. **P.P.C. Aucelli:** Validation, Supervision, Methodology, Formal analysis, Conceptualization.

Declaration of competing interest

The authors declare that they have no known competing financial interests or personal relationships that could have appeared to influence the work reported in this paper.

Data availability

Data is available within the article, in its supplementary materials, and at the link https://dist.altervista.org/seaproxy/.

Acknowledgement

The boreholes presented in this paper were made thanks to funding by the Coastal Demarcation Service of Cádiz (Spanish Ministry for the Ecological Transition and Demographic Challenge). This paper also benefited from the discussion at the Neptune (INQUA CMP project 2003P) and Onsea (INQUA CMP project 2404) meetings, and from the discussion at the meetings of the AIGeo (Associazione Italiana di Geografia Fisica e Gemorfologia) Working Group of Morfodinamica Costiera (2019-2023). This is a contribution to Research Group RNM-328 of the Andalusian Research Plan.

Appendix A. Supplementary data

Supplementary data to this article can be found online at https://doi.org/10.1016/j.geomorph.2024.109232.

References

Alberico, I., Amato, V., Aucelli, P.P.C., Di Paola, G., Pappone, G., Rosskopf, C.M., 2012. Historical and recent changes of the Sele River coastal plain (Southern Italy): natural variations and human pressures. Rendiconti Lincei 23 (1), 3–12. https://doi.org/10.1007/s12210-011-0156-y.

Allen, J.R.L., 2000. Morphodynamics of Holocene salt marshes: a review sketch from the Atlantic and Southern North Sea coasts of Europe. Quaternary Science Reviews 19, 1155–1231. https://doi.org/10.1016/S0277-3791(99)00034-7.

Alonso, C., Gracia, F.J., Benavente, J., 2004. Las marismas, alfares y salinas como indicadores para la restitución paleotopográfica de la Bahía de Cádiz durante la antigüedad. In: XVI Encuentros de Historia y Arqueología: Las industrias alfareras y conserveras fenicio-púnicas de la Bahía de Cádiz. Exmo, Ayuntamiento de San Fernando, pp. 263–287.

Alonso, C., Gracia, F.J., Benavente, J., 2009. Evolución histórica del sector meridional de la Bahía Interna de Cádiz. RAMPAS: Revista Atlántico-Mediterránea de Prehistoria y Arqueología Social 11, 13–37.

Alonso, C., Gracia, F.J., Rodríguez-Polo, S., Martín Puertas, C., 2015. El registro de eventos energéticos marinos en la Bahía de Cádiz durante épocas históricas. In: Rodríguez Vidal, J. (Ed.), Eventos energéticos marinos históricos y ocupación costera en el Golfo de Cádiz. Cuaternario y Geomorfología. https://doi.org/10.17735/cyg.v29i1-2.29935, 29 (1–2), 95–117.

Aranda, M., Gracia, F.J., Peralta, G., 2020. Estuarine mapping and eco-geomorphological characterization for potential application in conservation and management: three study cases along the Iberian coast. Appl. Sci. 10 (3), 4429. https://doi.org/10.3390/app10134429.

Arteaga, O.D., Schulz, H., Roos, A., 2008. Geoarqueología dialéctica en la Bahía de Cádiz. *Revista Atlántico-Mediterránea de Prehistoria y Arqueología Social* (RAMPAS, Universidad de Cádiz) 10, 21–116.

van Asselen, S., Cohen, K.M., Stouthamer, E., 2017. The impact of avulsion on groundwater level and peat formation in delta floodbasins during the middle-Holocene transgression in the Rhine-Meuse delta, the Netherlands. The Holocene 27, 1694–1706. https://doi.org/10.1177/0959683617702224.

van Asselen, S., Erkens, G., Stouthamer, E., Woolderink, H.A.G., Geeraert, R.E.E., Hefting, M.M., 2018. The relative contribution of peat compaction and oxidation to subsidence in built-up areas in the Rhine-Meuse delta, the Netherlands. Sci. Total Environ. 636, 177–191. https://doi.org/10.1016/j.scitotenv.2018.04.141.

Austermann, J., Mitrovica, J.X., Huyber, P., Rovere, A., 2017. Detection of a dynamic topography signal in last interglacial sea-level records. Sci. Adv. 3, e1700457 https://doi.org/10.1126/sciadv.1700457.

Bahr, D., Hutton, E.W.H., Syvitski, J.P.M., Pratson, L.F., 2001. Exponential approximations to compacted sediment porosity profiles. Comput. Geosci. 27 (6), 691–700.

The archaeology of Europe's drowned landscapes. In: Bailey, G., Galanidou, N., Peeters, H., Jöns, H., Mennenga, M. (Eds.), 2020. Coastal Research Library, 35. Springer Open, 560 pp.

Benavente, J., Del Río, L., Anfuso, G., Gracia, F.J., Nachite, D., Rodríguez Ramírez, A., Cáceres, L., 2007. Efecto de la marea en la clasificación morfodinámica de playas. In: Gómez Pujol, L., Fornós, J.J. (Eds.), Investigaciones recientes (2005–2007) en Geomorfología Litoral. Univ, Islas Baleares, IMEDEA-SEG, Palma de Mallorca, pp. 17–21.

Bernal-Casasola, D., Salomon, F., Díaz, J.J., Lara, M., Rixhon, G., Morales, J., Vidal, P., 2020. Deeper than expected: the finding of a remarkable ancient harbour at Gadir/Gades and an exceptional sedimentary archive (Cádiz, Southern Spain). J. Marit. Archaeol. 15, 165–183. https://doi.org/10.1007/s11457-020-09258-w.

Best, Ü.S.N., Van der Wegen, M., Dijkstra, J., Willemsen, P.W.J.M., Borsje, B.W., Roelvink, D.J.A., 2018. Do salt marshes survive sea level rise? Modelling wave action, morphodynamics and vegetation dynamics. Environ. Model. Software 109, 152–166. https://doi.org/10.1016/j.envsoft.2018.08.004.

Boski, T., Moura, D., Veiga-Pires, C., Camacho, S., Duarte, D., Scott, D.B. & Fernandes, S. G. (2002). Postglacial Sea-level rise and sedimentary response in the Guadiana Estuary, Portugal/Spain border, *Sedimentary Geology*, 150 (1–2), 103–122.

Boski, T., Camacho, S., Moura, D., Fletcher, W., Wilamowski, A., Veiga-Pires, C., Correia, V., Loureiro, C., Santana, P., 2008. Chronology of the sedimentary processes during the postglacial sea level rise in two estuaries of the Algarve coast, Southern Portugal. Estuar. Coast. Shelf Sci. 77 (2), 230e244 https://doi.org/10.1016/j.ecss.2007.09.012.

Bozi, B.S., Figueiredo, B.L., Rodrigues, E., Cohen, M.C.L., Pessenda, L.C.R., Alves, E.E.N., De Souza, A.V., Bendassolli, J.A., Macario, K., Azevedo, P., Culligan, N., 2021. Impacts of sea-level changes on mangroves from southeastern Brazil during the Holocene and Anthropocene using a multi-proxy approach. Geomorphology 390, 107860. https://doi.org/10.1016/j.geomorph.2021.107860.

Brain, M.J., Kemp, A.C., Horton, B.P., Culver, S.J., Parnell, A.C., Cahill, N., 2015. Quantifying the contribution of sediment compaction to late Holocene salt-marsh sea-level reconstructions, North Carolina, USA. Quatern. Res. 83, 41–51. https://doi.org/10.1016/j.yqres.2014.08.003.

Brisset, E., Burjachs, F., Navarro, B.J.B., de Pablo, J.F.L., 2018. Socio-ecological adaptation to Early-Holocene Sea-level rise in the western Mediterranean. Global Planet. Change 169, 156–167. https://doi.org/10.1016/j.gloplacha.2018.07.016.

Cáceres, L.M., Gómez, P., González-Regalado, M.L., Clemente, M.J., Rodríguez-Vidal, J., Toscano, A., Monge, G., Abad, M., Izquierdo, T., Monge Soares, A.M., Ruiz, F., Campos, J.M., Bermejo, J., Martínez-Aguirre, A., López, G.I., 2018. Modelling the mid-late Holocene evolution of the Huelva Estuary and its human colonization, South-Western Spain. Mar. Geol. 406, 12–26. https://doi.org/10.1016/j.margeo.2018.08.008.

Cahill, N., Kemp, A.C., Horton, B.P., Parnell, A.C., 2015. Modeling Sea-level change using errors-in-variables integrated Gaussian processes. Ann. Appl. Stat. 9 (2), 547–571. https://doi.org/10.1214/15-AOAS824.

Caporizzo, C., Aucelli, P.P.C., Galán-Ruffoni, I., Gracia, F.J., Martín-Puertas, C., Mattei, G., Stocchi, P., 2020. Estimating RSL changes in the Northern Bay of Cádiz (Spain) during the late Holocene. IMEKO TC-19 International Workshop on Metrology for the Sea 165–169.

Caporizzo, C., Gracia, F.J., Aucelli, P.P.C., Barbero, L., Martín-Puertas, C., Lagóstena, L., Ruiz, J.A., Alonso, C., Mattei, G., Galán-Ruffoni, I., López-Ramírez, J.A., Higueras-Milena, A., 2021. Late-Holocene evolution of the Northern Bay of Cádiz from geomorphological, stratigraphic and archaeological data. Quat. Int. 602, 92–109. https://doi.org/10.1016/j.quaint.2021.03.028.

Carrión-Torrente, A., Lobo, F.J., Puga-Bernabéu, A., Mendes, I., Lebreiro, S., García, M., Van Rooij, D., Luján, M., Reguera, M.I., Antón, L., 2022. Episodic postglacial deltaic pulses in the Gulf of Cádiz: Implications for the development of a transgressive shelf and driving environmental conditions. J. Sediment. Res. 92, 1116–1140.

Clark, J.A., Farrell, W.E., Peltier, W.R., 1978. Global changes in postglacial sea level: A numerical calculation. Quatern. Res. 9, 265–287. https://doi.org/10.1016/0033-5894(78)90033-9.

Corzo, R., 1980. Paleotopografía de la bahía gaditana. Gades 5, 5–14.

Dabrio, C.J., Zazo, C., Goy, J.L., Sierro, F.J., Borja, F., Lario, J., González, J.A., Flores, J. A., 2000. Depositional history of estuary infill during the last postglacial transgression (Gulf of Cadiz, Southern Spain). Mar. Geol. 162, 381–404.

De Boer, B., Van de Wal, R.S.W., Lourens, L.J., Bintanja, R., 2013. A continuous simulation of global ice volume over the past 1 million years with 3-D ice-sheet models. Climate Dynam. 41, 1365–1384. https://doi.org/10.1007/s00382-012-1562-2.

De Boer, B., Stocchi, P., Van De Wal, R., 2014. A fully coupled 3-D ice-sheet-sea-level model: algorithm and applications. Geosci. Model Dev. 7, 2141–2156. https://doi.org/10.5194/gmd-7-2141-2014.

Del Río, L., Benavente, J., Gracia, F.J., Alonso, C., Rodríguez Polo, S., 2015. Anthropogenic influence on spit dynamics at various timescales: Case study in the Bay of Cadiz (Spain). In: Randazzo, G., Jackson, D.W., Cooper, J.A.G. (Eds.), Sand and Gravel Spits, 12. Springer, Dordrecht, pp. 123–138. https://doi.org/10.1007/978-3-319-13716-2. Coastal Research Library.

Delgado, J., Boski, T., Nieto, J.M., Pereira, L., Moura, D., Gomes, A., Sousa, C., García-Tenorio, R., 2012. Sea-level rise and anthropogenic activities recorded in the late Pleistocene/Holocene sedimentary infill of the Guadiana Estuary (SW Iberia). Quaternary Science Reviews 33, 121–141. https://doi.org/10.1016/j.quascirev.2011.12.002.

Dyer, K.R., Christie, M.C., Wright, E.W., 2000. The classification of intertidal mudflats. Cont. Shelf Res. 20, 1039–1060. https://doi.org/10.1016/S0278-4343(00)00011-X.

Eckhardt, R., 1987. Stan Ulam, John von Neumann, and the Monte Carlo method. Los Alamos Science 15, 131–137.

Edwards, R.J., Horton, B.P., 2000. Reconstructing relative sea-level change using UK saltmarsh foraminifera. Mar. Geol. 169, 41–56. https://doi.org/10.1016/S0025-3227(00)00078-5.

Fa, D., Lario, J., Smith, P., Finlayson, J.C., 2000. Elementos sumergidos kársticos alrededor de la costa de Gibraltar y su potencial uso por humanos en la Prehistoria. In: Santiago Pérez, P., Martínez García, A., Mayoral Valsera, J. (Eds.), Actas I Congreso Andaluz de Espeleología. Federación Andaluza de Espeleología, Gibraltar.

Fagherazzi, S., Mariotti, G., Leonardi, N., Canestrelli, A., Nardin, W., Kearney, W.S., 2020. Salt marsh dynamics in a period of accelerated sea level rise. J. Geophys. Res. Earth 125 (8), e2019JF005200. https://doi.org/10.1029/2019JF005200.

Farrell, W.E., Clark, J.A., 1976. On postglacial sea level. Geophys. J. Roy. Astron. Soc. 46, 647–667. https://doi.org/10.1111/j.1365-246X.1976.tb01252.x.

Finkelstein, K., Ferland, M.A., 1987. Back-barrier response to sea-level rise, Eastern shore of Virginia. In: Nummedal, D., Pilkey, O.H., Howard, J.D. (Eds.), Sea-Level Fluctuation and Coastal Evolution. Society of Economic Paleontologists and Mineralogists, Tulsa, pp. 145–155.

García-Artola, A., Stéphan, P., Cearreta, A., Kopp, R.E., Khan, N.S., Horton, P., 2018. Holocene Sea-level database from the Atlantic coast of Europe. Quat. Sci. Rev. 196, 177–192. https://doi.org/10.1016/j.quascirev.2018.07.031.

Gómez, G., Ruiz, F., Rodríguez-Vidal, J., González-Regalado, M.L., Cáceres, L.M., Gómez, P., Abad, M., Izquierdo, T., Toscano, A., Arroyo, M., Romero, V., 2021. Miocene-late Quaternary environmental changes and molluscs as proxies of MIS-1 transgression in the Tinto-Odiel estuary, SW Spain. J. Iber. Geol. 48, 129–140. https://doi.org/10.1007/s41513-021-00183-y.

González-Acebrón, L., Mas, R., Arribas, J., Gutiérrez-Mas, J.M., Pérez-Garrido, C., 2016. Very coarse-grained beaches as a response to generalized sea level drops in a complex active tectonic setting: Pleistocene marine terraces at the Cadiz coast, SW Spain. Mar. Geol. 382, 92–110. https://doi.org/10.1016/j.margeo.2016.09.007.

Goy, J.L., Zazo, C., Dabrio, C.J., Lario, J., Borja, F., Sierro, F.J., Flores, J.A., 1996. Global and regional factors controlling changes of coastlines in Southern Iberia (Spain) during the Holocene. Quaternary Science Reviews 15, 773–780. https://doi.org/10.1016/S0277-3791(96)00071-6.

Gracia, F.J., Alonso, C., 2009. El cambiante paisaje de la bahía gaditana. In: Fernández-Palacios, J.M. (Ed.), Cádiz de la Constitución de 1812. Serie Agua, Territorio y Sociedad. Agencia Andaluza del Agua, Junta de Andalucía, pp. 28–31.

Gracia, F.J., Martín, C., 2009. Realización y datación de sondeos en la bahía de Cádiz y las marismas del Barbate. Ministerio de Medio Ambiente y Medio Rural y Marino, Cádiz, p. 116.

Gracia, F.J., Alonso, C., Gallardo, M., Giles, F., Benavente, J., López-Aguayo, F., 2000. Evolución eustática postflandriense en las marismas del Sur de la Bahía de Cádiz. Geogaceta 27, 71–74.

Gracia, F.J., Del Río, L., Alonso, C., Benavente, J., Anfuso, G., 2006. Historical evolution and present state of the coastal dune systems in the Atlantic coast of Cádiz (SW Spain): Palaeoclimatic and environmental implications. J. Coast. Res. SI 48, 55–63.

Gracia, F.J., Rodríguez-Vidal, J., Belluomini, G., Cáceres, L.M., Benavente, J., Alonso, C., 2008. Diapiric uplift of an MIS 3 marine deposit in SW Spain. Implications in late Pleistocene Sea level reconstruction and palaeogeography of the Strait of Gibraltar. Quaternary Science Reviews 27 (23–24), 2219–2231. https://doi.org/10.1016/j.quascirev.2008.08.013.

Gracia, F.J., Alonso, C., Giles, F., Benavente, J., Del Río, L., 2010. Evidencias del paso del río Guadalquivir por el interior de la Bahía de Cádiz durante el Pleistoceno Medio. In: Cuaternario y Arqueología. *Homenaje a Francisco Giles Pacheco*. Servicio de Publicaciones de la Diputación Provincial de Cádiz, pp. 9–17.

Gracia, F.J., Alonso, C., Abarca, J.M., 2017. Evolución histórica y geomorfología de las explotaciones salineras en marismas mareales. Ejemplos de la bahía de Cádiz. Cuaternario y Geomorfología 31 (1–2), 45–72. https://doi.org/10.17735/cyg.v31i1-2.54681.

Gracia, F.J., Alonso, C., Aparicio, J.A., 2022. The record of energetic marine events in the Bay of Cadiz during historical times. In: Álvarez, M., Machuca, F. (Eds.), Historical Earthquakes, Tsunamis and Archaeology in the Iberian Peninsula. Springer, Heidelberg, pp. 151–176. https://doi.org/10.1007/978-981-19-1979-4_7.

Gutiérrez-Mas, J.M., 2011. Glycymeris shell ac¬cumulations as indicators of recent sea-level changes and high-energy events in Cádiz Bay (SW Spain). Estuar. Coast. Shelf Sci. 92, 546–554. https://doi.org/10.1016/j.ecss.2011.02.010.

Gutiérrez-Mas, J.M., Juan, C., Morales, J.A., 2009. Evidence of high-energy events in shelly layers interbedded in coastal Holocene sands in Cadiz Bay (south-West Spain). Earth Surf. Process. Landf. 34, 810–823. https://doi.org/10.1002/esp.1770.

Hernández-Molina, F.J., Somoza, L., Rey, J., Pomar, L., 1994. Late Pleistocene-Holocene sediments on the Spanish continental shelves: model for very high-resolution sequence stratigraphy. Mar. Geol. 120, 129–174. https://doi.org/10.1016/0025-3227(94)90057-4.

Hijma, M.P., Engelhart, S.E., Törnqvist, T.E., Horton, B.P., Hu, P., Hill, D.F., 2015. A protocol for a geological sea-level database. In: Shennan, I., Long, A.J., Horton, B. P. (Eds.), Handbook of Sea-Level Research. Wiley Blackwell, pp. 536–553.

Hofstede, J.L.A., Becherer, J., Burchard, H., 2018. Are Wadden Sea tidal systems with a higher tidal range more resilient against sea level rise? J. Coast. Conserv. 22, 71–78. https://doi.org/10.1007/s11852-016-0469-1.

Karkani, A., Evelpidou, N., Giaime, M., Marriner, N., Morhange, C., Spada, G., 2019. Late Holocene Sea-level evolution of Paros Island (Cyclades, Greece). Quat. Int. 500, 139–146. https://doi.org/10.1016/j.quaint.2019.02.027.

Khan, N.S., Ashe, E., Shaw, T.A., Vacchi, M., Walker, J., Peltier, W.R., Kopp, R.E., Horton, B.P., 2015. Holocene relative sea-level changes from near-, intermediate-, and far-field locations. Curr. Clim. Chang. Rep. 1, 247–262. https://doi.org/10.1007/s40641-015-0029-z.

Khan, N.S., Horton, B.P., Engelhart, S., Rovere, A., Vacchi, M., Ashe, E.L., Törnqvist, T.E., Dutton, A., Hijma, M.P., Shennan, I., 2019. Inception of a global atlas of sea levels since the last Glacial Maximum. Quaternary Science Reviews 220, 359–371. https://doi.org/10.1016/j.quascirev.2019.07.016.

Kirwan, M.L., Guntenspergen, G.R., D'Alpaos, A., Morris, J.T., Mudd, S.M., Temmerman, S., 2010. Limits on the adaptability of coastal marshes to rising sea level. Geophys. Res. Lett. 37, L23401 https://doi.org/10.1029/2010GL045489.

Kirwan, M.L., Temmerman, S., Skeehan, E.E., Guntenspergen, G.R., Fagherazzi, S., 2016. Overestimation of marsh vulnerability to sea level rise. Nat. Clim. Chang. 24, 253–260. https://doi.org/10.1038/NCLIMATE2909.

Kopp, R.E., Hay, C.C., Little, C.M., Mitrovica, J.X., 2015. Geographic variability of sea-level change. Current Climate Change Reports 1, 192–204. https://doi.org/10.1007/s40641-015-0015-5.

Lario, J. (1996). *Último y Presente Interglacial en el área de conexión Atlántico-Mediterráneo. Variaciones del nivel del mar, paleoclima y paleoambientes*. PhD Thesis, Univ. Complutense de Madrid, Madrid, 269 p. (In Spanish).

Leorri, E., Cearreta, A., Milne, G., 2012. Field observations and modelling of Holocene Sea-level changes in the southern Bay of Biscay: implication for understanding current rates of relative sea-level change and vertical land motion along the Atlantic coast of SW Europe. Quaternary Science Reviews 42, 59–73. https://doi.org/10.1016/j.quascirev.2012.03.014.

Llave, E., Hernández-Molina, F.J., Alonso, C., Gallardo, M., Vázquez, J.T., López-Aguayo, F., 1999. Caracterización y evolución del paleocauce del río Guadalete en la Bahía de Cádiz durante el Cuaternario terminal. Geogaceta 26, 43–46.

Lobo, F.J., Hernández-Molina, F.J., Somoza, L., Díaz del Río, V., 2001. The sedimentary record of the postsd-glacial transgression on the Gulf of Cadiz continental shelf (Southwest Spain). Mar. Geol. 178, 171–195. https://doi.org/10.1016/S0025-3227(01)00176-1.

Lobo, F.J., Fernández-Salas, L.M., Hernández-Molina, F.J., González, R., Dias, J.M.A., Díaz del Río, V., Somoza, L., 2005. Holocene highstand deposits in the Gulf of Cadiz, SW Iberian Peninsula: A high-resolution record of hierarchical environmental changes. Mar. Geol. 219, 109–131. https://doi.org/10.1016/j.margeo.2005.06.005.

López-Sáez, J.A., Pérez-Díaz, S., Rodríguez-Ramírez, A., Blanco-González, A., Villarías-Robles, J.J.R., Luelmo-Lautenschlaeger, R., Jiménez-Moreno, G., Celestino-Pérez, S., Cerrillo-Cuenca, E., Pérez-Asensio, J.N., León, A., 2018. Mid-late Holocene environmental and cultural dynamics at the south-west tip of Europe (Doñana National Park, SW Iberia, Spain). J. Archaeol. Sci. Rep. 22, 58–78. https://doi.org/10.1016/j.jasrep.2018.09.014.

Losada, M.A., Baquerizo, A., Ortega-Sánchez, M., Ávila, A., 2011. Coastal evolution, sea level and assessment of intrinsic uncertainty. *Journal of Coastal Research*, S.I. 59, 218–228.

Martínez-Sánchez, A., Gracia, F.J., Alonso, C., Mata, E., Caporizzo, C., 2023. Reconstructing the historical shoreline evolution of the Northern Bay of Cádiz (SW

Spain) from geomorphological and geoarchaeological data. J. Maps. https://doi.org/10.1080/17445647.2023.2206585.
Martins, J.M.M., Soares, A.M.M., 2013. Marine Radiocarbon Reservoir effect in Southern Atlantic Iberian Coast. Radiocarbon 55 (2–3), 1123–1134. https://doi.org/10.1017/S0033822200048037.
Mattei, G., Rizzo, A., Anfuso, G., Aucelli, P.P.C., Gracia, F.J., 2019. A tool for evaluating the archaeological heritage vulnerability to coastal processes: the case study of Naples Gulf (southern Italy). Ocean & Coastal Management 179, 104876. https://doi.org/10.1016/j.ocecoaman.2019.104876.
Mattei, G., Caporizzo, C., Corrado, G., Vacchi, M., Stocchi, P., Pappone, G., Schiattarella, M., Aucelli, P.P.C., 2022. On the influence of vertical ground movements on Late-Quaternary Sea-level records. A comprehensive assessment along the mid-Tyrrhenian coast of Italy (Mediterranean Sea). Quaternary Science Reviews 279. https://doi.org/10.1016/j.quascirev.2022.107384.
May, S.M., Brückner, H., Norpoth, M., Pint, A., Wolf, D., Brill, D., León Martín, C., Stika, H.-P., Suárez, J., Moret, P., Marzoli, D., 2022. Holocene coastal evolution and environmental changes in the lower Río Guadiaro valley, with particular focus on the Bronze to Iron Age harbour "Montilla" of Los Castillejos de Alcorrín (Málaga, Andalusia, Spain). Geoarchaeology 38, 129–155. https://doi.org/10.1002/gea.21943.
Mediavilla, R., Antón-López, L., Dabrio, C.J., Perucha, M.A, Santisteban, J.I., Mediato, J. F., Barnolas, A. & Llave, E. (2004). Distribución y caracterización de los depósitos fluviales pleistocenos del subsuelo de la Bahía de Cádiz. Geotemas, 6(5): 203–206.
Milne, G.A., Mitrovica, J.X., 2008. Searching for eustasy in deglacial sea-level histories. Quat. Sci. Rev. 27, 2292–2302. https://doi.org/10.1016/j.quascirev.2008.08.018.
Mitrovica, J.X., Peltier, W.R., 1993. The inference of mantle viscosity from an inversion of the Fennoscandian relaxation spectrum. Geophys. J. Int. 114 (1), 45–62. https://doi.org/10.1111/j.1365-246X.1993.tb01465.x.
Morales, J.A., San Miguel, E.G., Borrego, J., 2003. Tasas de sedimentación reciente en la Ría de Huelva. Geogaceta 33, 15–18.
Nageswara Rao, K., Pandey, S., Kubo, S., Saito, Y., Kumar, K.Ch.V.N., Demudu, G., Hema Malini, B., Nagumo, N., Nakashima, R., Sadakata, N., 2020. Paleoclimate and Holocene relative sea-level history of the east coast of India. J. Paleolimnol. 64, 71–89. https://doi.org/10.1007/s10933-020-00124-2.
Nelson, Alan R., 2015. Coastal Sediments. Handbook of Sea-Level Research, pp. 47–65.
Niveau de Villedary, A.M., Ruiz Mata, D., 1995. El poblado de Las Cumbres (Castillo de Doña Blanca). Urbanismo y materiales del siglo III a.C. Actas del IV Congreso internacional de estudios fenicios y púnicos, Cádiz, Spain 893–903, 2–6 octubre.
Pappone, G., Aucelli, P.P.C., Alberico, I., Amato, V., Antonioli, F., Cesarano, M., Di Paola, G., Pelosi, N., 2012. Relative Sea-level rise and marine erosion and inundation in the Sele river coastal plain (Southern Italy): scenarios for the next century. Rendiconti Lincei. 23, 121–129. https://doi.org/10.1007/s12210-012-0166-4.
Peltier, W.R., 1976. Glacial isostatic adjustment - II: the inverse problem. Geophys. J.R. Astron. Sot. 46, 669.
Peltier, W.R., 2004. Global Glacial Isostasy and the Surface of the Ice-Age Earth: the ICE-5G (VM2) model and GRACE. Annual Reviews. Earth Planet. Sciences 32, 111–149. https://doi.org/10.1146/annurev.earth.32.082503.144359.
Peltier, W.R., Argus, D.F., Drummond, R., 2015. Space geodesy constrains ICE-age terminal deglaciation: the global ICE-6G_C (VM5a) model. J. Geophys. Res. Solid Earth 120, 450–487. https://doi.org/10.1002/2014JB011176.
Ponce Cordones, F., 1985. Consideraciones en torno a la ubicación del Cádiz fenicio. Anales de la Universidad de Cádiz II, 99–121.
Rahman, R., Plater, A.J., 2014. Particle-size evidence of estuary evolution: A rapid and diagnostic tool for determining the nature of recent saltmarsh accretion. Geomorphology 213, 139–152. https://doi.org/10.1016/j.geomorph.2014.01.004.
Reed, D., Wang, Y., Meselhe, E., White, E., 2020. Modelling wetland transitions and loss in coastal Louisiana under scenarios of future relative sea-level rise. Geomorphology 352, 106991. https://doi.org/10.1016/j.geomorph.2019.106991.
Rodríguez Polo, S., Gracia, F.J., Benavente, J., Del Río, L., 2009. Geometry and recent evolution of the Holocene beach ridges of the Valdelagrana littoral spit (Cádiz Bay, SW Spain). *Journal of Coastal Research*, S.I. 56, 20–23.
Rodríguez-Ramírez, A., Villarías-Robles, J.J.R., Pérez-Asensio, J.N., Santos, A., Morales, J.A., Celestino-Pérez, S., León, A., Santos-Arévalo, F.J., 2016. Geomorphological record of extreme wave events during Roman times in the Guadalquivir estuary (Gulf of Cádiz, SW Spain): an archaeological and paleogeographical approach. Geomorphology 261, 103–118. https://doi.org/10.1016/j.geomorph.2016.02.030.
Rodríguez-Ramírez, A., Villarías-Robles, J.J.R., Pérez-Asensio, J.N., Celestino-Pérez, S., 2019. The Guadalquivir Estuary: Spits and marshes. In: Morales, J.A. (Ed.), The Spanish Coastal Systems. Springer Nature, pp. 517–541. https://doi.org/10.1007/978-3-319-93169-2_22.
Rovere, A., Stocchi, P., Vacchi, M., 2016a. Eustatic and Relative Sea Level changes. Current.Climate Change Reports 2, 221–231. https://doi.org/10.1007/s40641-016-0045-7.
Rovere, A., Raymo, M.E., Vacchi, M., Lorscheid, T., Stocchi, P., Gómez-Pujol, L., Harris, D.L., Casella, E., O'Leary, M.J., Hearty, P.J., 2016b. The analysis of last Interglacial (MIS 5e) relative sea-level indicators: Reconstructing Sea-level in a warmer world. Earth Sci. Rev. 159, 404–427. https://doi.org/10.1016/j.earscirev.2016.06.006.
Rovere, A., Pico, T., Richards, F., O'Leary, M.J., Mitrovica, J.X., Goodwin, I.D., Austermann, J., Latychev, K., 2023. Influence of reef isostasy, dynamic topography, and glacial isostatic adjustment on sea-level records in Northeastern Australia. Commun. Earth Environ 4, 328. https://doi.org/10.1038/s43247-023-00967-3.
Roy, K., Peltier, W.R., 2018a. Relative Sea level in the Western Mediterranean basin: a regional test of the ICE-7G_NA (VM7) model and a constraint on late Holocene Antarctic deglaciation. Quaternary Science Reviews 183, 76–87. https://doi.org/10.1016/j.quascirev.2017.12.021.
Roy, K., Peltier, W.R., 2018b. Relative Sea level in the Western Mediterranean basin: A regional test on the ICE-7G_NA (VM7) model and a constraint on late Holocene Antarctic deglaciation. Quaternary Science Reviews 183, 76–87. https://doi.org/10.1016/j.quascirev.2017.12.021.
Ruiz Mata, D., 1999. La fundación de Gadir y el Castillo de Doña Blanca: contrastación textual y arqueológica. Complutum 10, 279–317.
Salomon, F., Bernal-Casasola, D., Díaz, J.J., Lara, M., Domínguez-Bella, S., Ertlen, D., Wassmer, P., Adam, P., Schaeffer, P., Hardion, L., Vittori, C., Chapkanski, S., Delile, H., Schmitt, L., Preusser, F., Trautmann, M., Masi, A., Vignola, C., Sadori, L., Morales, J., Vidal Matutano, P., Robin, V., Keller, B., Sanchez, Bellón, A., Martínez López, J., Rixhon, G., 2020. High-resolution late Holocene sedimentary cores record the long history of the city of Cádiz (South-Western Spain). Sci. Drill. 27, 35–47. https://doi.org/10.5194/sd-27-35-2020.
Sampath, D.M.R., Boski, T., Loureiro, C., Sousa, C., 2015. Modellilng of estuarine response to sea-level rise during the Holocene: Application to the Guadiana Estuary-SW Iberia. Geomorphology 232, 47–64. https://doi.org/10.1016/j.geomorph.2014.12.037.
Shennan, I. (2003). Relative Sea-level change in Great Britain: Observations, tidal and glacio-hydro-isostatic modelling and the broader implications for sea-level research. In: *Coastal Environmental Change during Sea-Level Highstands: A Global Synthesis with implications for management of future coastal change*. Project IGCP 437 Final Conference, Puglia. Otranto/Taranto, p. 213-214.
Shennan, I., Horton, B., 2002. Holocene land- and sea-level changes in Great Britain. J. Quat. Sci. 17 (5–6), 511–526. https://doi.org/10.1002/jqs.710.
Shennan, I., Long, A.J., Horton, B.P. (Eds.), 2015. Handbook of Sea-Level Research. John Wiley and Sons, Chichester, West Sussex, UK. https://doi.org/10.1002/9781118452547.
Sousa, C., Boski, T., Pereira, L., 2019. Holocene evolution of a barrier island system, Ria Formosa, South Portugal. The Holocene 29, 64–76. https://doi.org/10.1177/0959683618804639.
Spada, G., Stocchi, P., 2007. SELEN: a Fortran 90 program for solving the "Sea Level Equation". Comput. Geosci. 33, 538. https://doi.org/10.1016/j.cageo.2006.08.006.
Stanford, J.D., Hemingway, R., Rohling, E.J., Challenor, P.G., Medina-Elizalde, M., Lester, A.J., 2011. Sea-level probability for the last deglaciation: A statistical analysis of far-field records. Global Planet. Change 79 (3–4), 193–203. https://doi.org/10.1016/j.gloplacha.2010.11.002.
Stanley, D.J., 1995. A global sea-level curve for the late Quaternary: the impossible dream? Mar. Geol. 125, 1–6.
Stocchi, P., Vacchi, M., Lorscheid, T., de Boer, B., Simms, A.R., Van de Wal, R.S.W., Vermeersen, B.L.A., Pappalardo, M., Rovere, A., 2018. MIS 5e relative sea-level changes in the Mediterranean Sea: Contribution of isostatic disequilibrium. Quaternary Science Reviews 185, 122–134. https://doi.org/10.1016/j.quascirev.2018.01.004.
Stuiver, M., Reimer, P.J., Reimer, R.W., 2021. CALIB 8.2 [WWW program] at. http://calib.org. (Accessed 5 January 2021).
Talavera, L., Del Río, L., Benavente, J., Barbero, L., López-Ramírez, J.A., 2018. UAS as tools for rapid detection of storm-induced morphodynamic changes at Camposoto beach, SW Spain. Int. J. Remote Sens. 39, 5550–5567. https://doi.org/10.1080/01431161.2018.1471549.
Teixeira, S.B., Gaspar, P., Rosa, M. (2005). Holocene Sea-level index points on the Quarteira Coast (Algarve, Portugal). In: Freitas, M.C., Drago, T. (Eds.), Iberian Holocene Paleoenvironmental Evolution. Proceedings Coastal Hope Conference 2005, Universidade de Lisboa, pp. 125–127.
Turney, C.S.M., Brown, H., 2007. Catastrophic early Holocene Sea level rise, human migration and the Neolithic transition in Europe. Quaternary Science Reviews 26, 2036e2041. https://doi.org/10.1016/j.quascirev.2007.07.003.
Vacchi, M., Marriner, N., Morhange, C., Spada, G., Fontana, A., Rovere, A., 2016. Multiproxy assessment of Holocene relative sea-level changes in the western Mediterranean: Sea-level variability and improvements in the definition of the isostatic signal. Earth-Science Reviews 155, 172–197. https://doi.org/10.1016/j.earscirev.2016.02.002.
Zazo, C., Dabrio, C.J., Goy, J.L., Lario, J., Cabero, A., Silva, P.G., Bardají, T., Mercier, N., Borja, F., Roquero, E., 2008. The coastal archives of the last 15 ka in the Atlantic-Mediterranean Spanish linkage area: Sea level and climate changes. Quat. Int. 181, 72–87. https://doi.org/10.1016/j.quaint.2007.05.021.